Evaluating the Sample Size for LIBS characterization in Mining Operations

19 November 2018

SPECTRAL
INDUSTRIES

TUDelft

Chris (C.H.J.) Elpenhof
4228693

Abstract

In the mining industry, sampling is an essential feature for the characterization of the material when all available material cannot be examined and only a small fraction of the total is evaluated. This study addresses how the minimum number of samples required to obtain a statistically accurate answer. This is important since less sample measurement save time and money. The sample size is related to the homo- and heterogeneity of a rock sample, where the sample size of a homogeneous material is smaller than a heterogeneous material.

Many types of research is carried out on the sampling theory, but it is hard to create a formula to determine the sample size beforehand based on a rate of heterogeneity. The homogeneity percentage is not linked to the sample size, but with a spatial elemental distribution, this can be possible. However, further research is needed in order to answer the question more exact for a situation that is more complex. This study first mentions several definitions of homogeneity, second their origin within geology is evaluated. Last this is calculated with theoretical models to explore the minimum sample size required.

The project evaluates how the sample size changes when homogeneity, heterogeneity and spatial distribution of the grade varies within a rock image. It is done with the help of an image analysis tool which creates a homogeneity curve, the mean and standard deviations for an increasing sample size. The standard deviations are used to generate answer within different levels of confidence for certain margins of error.

Also, the variogram is used to determine the spatial correlation of the sample and interpolation is made using a general kriging method. Multiple images are evaluated with different rates of homogeneity, the number of elements and their spatial distribution. This study proofs generating more samples increases the accuracy of the characterization. With a lower target grade, the sample size will increase and also with an increasing image or grid size the number of samples will decrease. The variogram gives a first impression of the homogeneity since a smaller range and sill indicates more homogeneous material.

Contents

1. Introduction

The characterization of ore in a mining environment is becoming more and more critical. Mostly it is carried out before any processing steps have taken place whereby quantity, grade or quality, densities, shape, and physical characteristics are determined to allow for the appropriate application of technical and economic parameters to support production planning and evaluation of the economic viability of deposits [1].

Ore reserves and grades are declining each year around the world, mainly due to massive mining and the need of the minerals. Due to more complex and extensive formations, it is becoming more challenging to mine high-grade minerals. Therefore, sufficient characterization of elements in the mineral is needed to assess, for example, the grade and classification of waste and ore material. Nowadays, this is already happening with multiple techniques like XRF, but these are in most of the cases, not the fastest.

Laser-Induced Breakdown Spectroscopy (LIBS) is a well-known technique for elemental characterization. With LIBS the characterization time of the elements can be decreased, which make the costly and time-consuming laboratory analysis secondary in the decision making of the exploration phase [2]. This method can be applied for drilling cuttings or in drill hole samples, but also in activities not related to the mining industry.

This study investigates the sample size of the LIBS spectroscopy in the mining industry for elemental determination. It is usually impossible to characterize all material available, so one is always dependent on taking a representative sample for any element. Here, the relation between heterogeneity/homogeneity and the sample size will be investigated, since it may have severe complications for characterizing the elemental composition of the ore.

First, LIBS characterization will be evaluated, where after several theoretical concepts for assessing homo- and heterogeneity will be discussed. Next, multiple case studies are carried out to evaluate the required sample size within different situations. Last, the results will be discussed and a conclusion will be given.

1.1 Spectral Industries

This study is carried out in correspondence with Spectral Industries which is a young high-tech company that develops instrumentation for chemical sensing based on optical spectroscopy. Their applications are in the mining and recycling industry, in agriculture, but also in any research and development lab that needs real-time analysis of chemical composition. They focus on LIBS, a laser-based atomic emission technique where the focus market lies within the mining industry.

They also contribute to the real-time mining project, a European collaboration in the field of real-time mining between fifteen partners from five different countries. The aim is to develop a real-time framework to decrease environmental impact and increase resource efficiency in the raw material extraction industry for Europe. For this research, in-situ and sensor-based ore characterization methods are evaluated. The geological parameters that are to be identified include texture, mineralogy, and geochemistry [3].

1.2 LIBS spectroscopy

LIBS is an analytical method that has been evaluated in substantial researches over the last 25 years. The typical setup can be found in Figure 1. It consists out of a laser which generates pulsed light. It includes a beam-shaping mechanism and steering optics, which can be a lens. With the help of collection optics, a spectrograph, and a wavelength-sensitive detector the plasma light can be measured. LIBS is operated using a high-energy pulses laser, which uses tens to hundreds of mJ per pulse and using the focusing lens it will generate a plasma where a little volume of the sample will be vaporized [4]. A portion of the plasma is dispersed by a spectrometer after which the detector records the emission signals. After digitalizing the signal, the data is displayed for the intensity and the wavelength components.
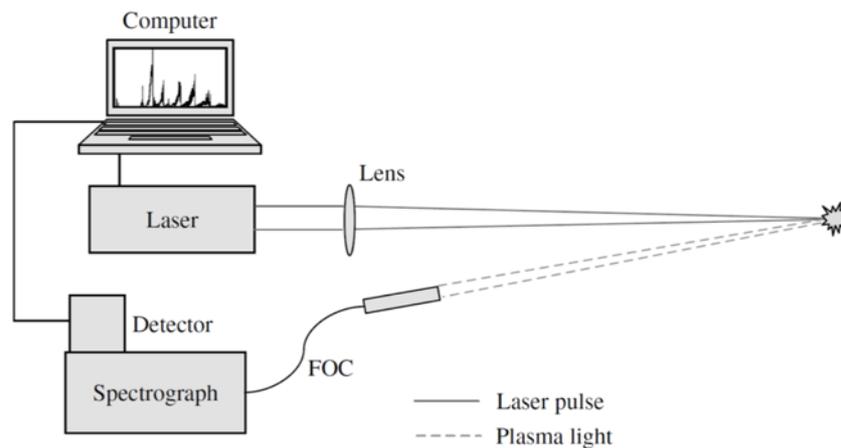
Figure 1. Basic understanding of a simplified LIBS setup [21].

Using this signal, interpretation of the minerals can be done. Characteristic elemental information is available in a database containing mineral reference spectra for most of the elements. On average, the spectra are broad bands reaching from 200nm to 800nm [2].

As an example, Figure 2 shows the atomic transition lines for hematite (Fe_2O_3) and chalcopyrite ($CuFeS_2$) minerals. Both minerals have similar intensity peaks at the same wavelength, which indicates a similarity in iron. Differences in wavelength are shown in the 510-521nm range, which discovers the variances between hematite and chalcopyrite. The same peaks are visible for 486nm, 488nm, 491nm, 495nm due to having iron in common. The differences are at 510m, 515nm, 521nm for Chalcopyrite and 513nm, 516nm and 519nm for Hematite.
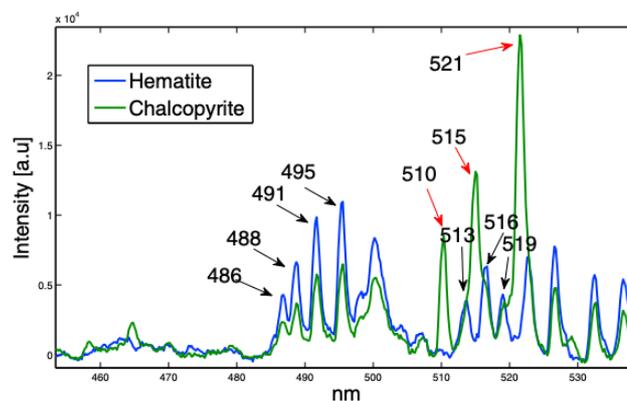
Figure 2. Atomic transition lines selected as indicators for hematite and chalcopyrite [2].

Comparing LIBS with other methods of atomic emission spectroscopy, its two significant advantages are that time-consuming sample preparation is not necessary and measurements can be done rapidly, which means several seconds instead of minutes, comparing it with XRF [5]. Also, elements with an atomic number less than twenty can be detected. A significant disadvantage is that the sample excitation conditions are sensitive to variation in laser parameters and characteristics of the sample, which will limit the analytical performance [5].

1.3 LIBS for mineral characterization

In the mining industry, mineral identification can provide valuable and essential information. It is stated that LIBS is a powerful and useful way to analyse the chemical compound of a subject. In this study, LIBS is needed to characterize mineral compounds. In several articles, LIBS is stated as a widely applied online surface scanning technique, unless some mineral groups cannot be determined yet [2].

LIBS has shown already promising results for characterization the quality of a spectrum of ore types including iron ore, copper ore, uranium ore, phosphate ore, nickel laterite, and coal [6]. The main problem with mineral characterization is that in an online system, heterogeneity of the material is problematic. In most of the researches focused on the utilization of LIBS, sample preparations have been carried out to make it homogeneous in the form of a powder or a pellet [6]. Only phosphate ore and coal are possible ores for online determination with the use of a LIBS sensor [7].

As mentioned before, heterogeneity is a significant concern for determining the elemental composition of an ore. It is expected that increasing the sample size will decrease the sampling error. However, it preferred to have a sample size as small as possible. To go into this more in-depth, the hetero- and homogeneity will be discussed.

2. Geological influence

For LIBS measurements, the homo- and heterogeneity are very important for the sample size. LIBS can be used for a wide variety of activities. If it is used for separation of different alloys of aluminium, it is likely that one hit per sample is enough for a valid characterization. The sample size is low since the material is human-made and assumed to be homogeneous throughout the whole surface and volume of the material. For characterization of rocks, this is different. The material is not man-made but is created over millions of years and shaped and reshaped multiple times. It is a natural product where nobody will know the exact composition until further research has been carried out. Therefore, geological factors and activity are the main reason causing heterogeneity in a material.

When characterizing a rock sample for its composition, knowing what kind of material is dealt with can make considerable importance to the number of samples needed for sufficient characterization. The structure of formations can give vital information about the heterogeneity of the material. As can be seen in Figure 3, eight examples are presented with different structures. At first sight, the obsidian can be categorized as homogeneous. The calico and banded gneiss are also homogeneous, but only in a particular direction due to their laminated structure. Breccia and coquina are coarse-grained and therefore more heterogeneous. Serpentine, talc schist and porphyry structures behave heterogeneously. Especially the porphyry structure, where a certain consistency can be observed.

From a first impression of the material, an idea for the required number of samples needed for characterization can be assessed. In the mining industry this is always done beforehand since it is unlogic and precarious to start digging at a random location hoping a valuable material will be discovered. In current mining industries, this is not possible since valuables occur as a trace element and are most of the time invisible [6].

Figure 3. Samples of different rock types. The varying composition and geological structures can be seen [27].

Within geology, three main types of rocks are distinguished; 1) igneous, 2) metamorphic and 3) sedimentary rocks. Igneous rocks form from the cooling of magma inside the earth and often have large crystals. Metamorphic rocks are formed through the change of igneous and sedimentary rocks, and sedimentary rocks are formed through solidification of sediment which can have an origin of organic remain or from cementing debris of other rocks.

Within these types of rocks, certain elements are often characteristic for the lot. If a particular mineral is found, it can be correlated with another mineral so one can assume those other minerals can also be found within the material, which is making use of certain trace elements. However, this is also speculation since one cannot know what is inside of rock without doing proper research on the composition.

As seen in Figure 3, a variety of structures are known. One can say that for the three types of rock described above a typical composition can be assumed. Sedimentary rocks have a typical occurrence of layers, while metamorphic rocks can have quite a homogeneous appearance due to extensive mineralization with a widespread speckled surface but they also occur with a layered or laminated structure so an overall representation cannot be made. Igneous rocks like diorite are often relatively homogenous due to their equally divided mineralization. However, an assumption can be made for some variation in the structures of these rocks, and it is about all the structures within these categories. Many geological factors can have changed the materials composition so a normalization cannot be made.

From the images in Figure 3 it can be seen that varieties of structures are possible and that different types of rocks require different sample size to be characterized. Next, sample size itself will be discussed and the level of confidence and margin of error will be introduced. In the end of this study, case studies will be carried out which are similar to Figure 3.

3. Sample size

As mentioned, the primary type of sampling error is known as the fundamental sampling error (FSE), defined by Gy (1979). These errors explain the precision and accuracy of the data, which is shown in Appendix A. For a given material, some samples will be taken to characterize the material. The factors of precision and accuracy have a significant influence and the sample results, comparing this with the composition of the population.
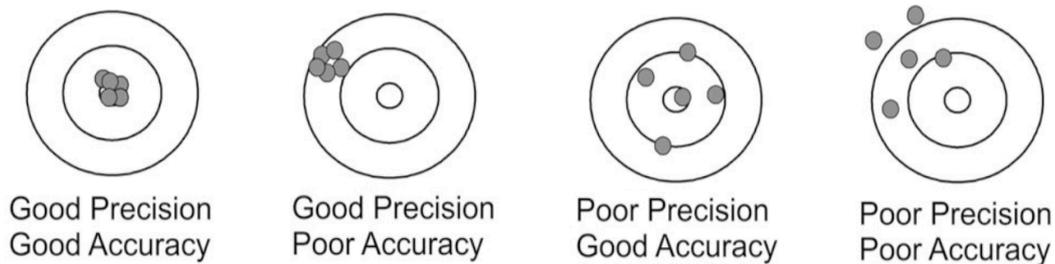
Figure 4. Definition of the concepts of precision and accuracy [8].

Precision is a measure of how close sample values are to each other and accuracy is a measure of how close the sample value is comparing it with the true grade [8]. In characterization, the accuracy and precision are essential, since one wants to know the composition of a certain material. Unfortunately, in LIBS measurements it is not possible to know in front what the material is, so it is much harder to know the precision and accuracy beforehand. If the whole composition is known, assumption can be made, but in most cases, this is not possible.

For LIBS measurements, ideally, it would be good to know the number of measurements needed to get information at a certain level of confidence. The access the variance of a sample, determination of several parameters is mandatory. Otherwise, no assumptions can be made since it is not possible to assume a certain sample size without any boundary conditions.

For this research, the aim is to answer the question of how many samples are needed to determine a material within a certain level of confidence. Various possibilities are tried and investigated to evaluate the hetero- and homogeneity of theoretical and real-life samples. Since hetero- and homogeneity are the most significant factors contributing to the level of uncertainty in sampling, it will be tried to find a correlation between homogeneity and sampling size.

Defining the sample size, two parameters are fundamental; 1) the margin of error and 2) the level of confidence. The margin of error is the level of precision that one requires for the results of the sample measurements and can be absolute or relative, which will be explained in a later section. It is the range in which the characterization of a material that is tried to be measured is estimated. Most of the times it is expressed as a percentage, as ±3%. It is commonly accepted that for decreasing the margin of error, the sample size needs to be increased, but that will be evaluated in the following paragraphs.

The confidence level is linked to the confidence interval, since the higher the confidence level, the wider the interval will be. The confidence level is the percentage of all possible samples that can be expected to include a true population parameter. For example, a poll might state there is a 95% confidence level of 4.88 and 5.26. This means if the poll is repeated using the same techniques, 95% of the time the true population parameter will fall within the interval estimates 95% of the time. An example if the margin of error is equal to three percentage points, with mean of 35%, measurements will be within 32% and 38%, 95% of the time.

Figure 5 gives an overview of the 68%, 95% and 99.7% related to the standard deviation and the mean of a given dataset.
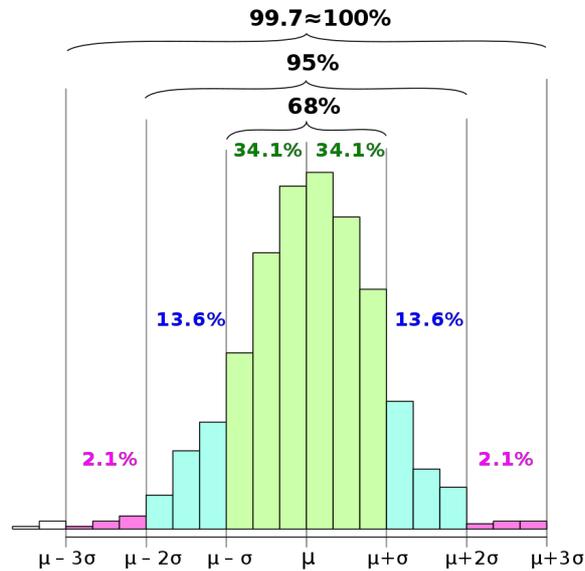
Figure 5. Overview where the 68%, 95% and 99.7% confidence intervals can be seen, related to the standard deviation [26].

This is used to define the confidence level for a LIBS dataset, within a certain range from the mean of the measurements. For a 95% confidence interval, the measurements lie within two standard deviations from the mean. For 68% and 99.7%, these are respectively one and three standard deviations. For LIBS measurements, the standard deviation needs to be as small as possible in order to be within a range of, for example, 95%, because this will increase the accuracy. Logically, this is related to the sample size, and this study will evaluate the number of samples needed for a specific representation of the total image or population. The margin of error will be later be used to examine the required minimal sample size.

3.1 Sample size for a known population

The sample size for a given population can be calculated using the Cochran's sample size formula for categorical data. The number of samples can be calculated with different margins of error and variances. To do so, the following formula is used [9];

$$n = \frac{\dfrac{\underline{\underline{z}}^2 * (p)(q)}{\underline{e}^2}}{\left(1 + \dfrac{\underline{\underline{z}}^2 * (p)(q)}{population * \underline{e}^2}\right)}$$

Here, *z* is the selected alpha level for each tail in the Gaussian distribution. It corresponds to the level of confidence for evaluating the population. The values for *z* can be found in Table 1. *(p)(q)* is the estimate of the variance; for a maximum possible proportion, *p* is equal to 0.5. *q* is equal to 1-0.5 = 0.5. p and q are the maximum possible proportion of the population, which is equal to 0.5. For two parameters, the change of sampling the target is 50%/50%, which explains the value for p and q. This produces the maximum possible sample size. *e* is the acceptable margin of error for the proportion.

Table 1. Values for z with their corresponding confidence level.

Level of confidence	80%	90%	95%	98%	99%
z	1.28	1.645	1.96	2.33	2.58

For example, if a grid of 50x50 pixel^2 is evaluated, the population size is equal to 2500. Using a level of confidence of 95%, a margin of error of 5% and a proportion of 50%, the sample size is equal to 333.

$$n = \frac{\dfrac{1.96^2 * (0.5)(1-0.5)}{0.05^2}}{(1 + \dfrac{1.96^2 * (0.5)(1-0.5)}{2500 * 0.05^2})} = 333$$

According to Cochran, for a population of 2500, 333 samples are needed to evaluate with of 95% level of confidence and a 5% margin of error. This indicates a sample size of 13.3% of the total grid size. It can be questioned if this is indeed true, since it is expected the distribution of the sample will contribute also to determination of the sample size. Appendix C provides an overview of the formula that finds the smallest sample size providing the desired level of precision.

4. Homo- and heterogeneity

Sensor-based sorting is one of the most critical parts in the processing of minerals. Typically, there are two sensors, one that measures a characteristic of the bulk of a particle and one measure a property of the surface of a particle [10]. LIBS measurements are categorized within the last group, where the surface measurement needs to be correlated to the bulk property of the material. Therefore, it needs to be analysed how well the surface correlates with the volume of the material. Intraparticle is one of the critical parameters linked to the correlation since it defines heterogeneity within each particle.

Heterogeneity is created by geological processing that has taken place during the formation of the orebody. The first step in order to define a specific heterogeneity can be achieved by understanding the lithologies within the orebodies since specific lithologies often correspond with a typical elemental composition. The elemental composition is often related to the heterogeneity of the material since more elements often mean a higher heterogeneity.

Pure homogeneity is assumed to have 1) a unique mineralogy with 2) all grains of similar shapes and sizes with 3) no spatial organization or patterns present [11]. Figure 6 gives an overview of the two components of heterogeneity, which consists out of grain components and spatial fabric and how the two components are build up.

4.1 Scaling

One of the most important parameters related to hetero- and homogeneity is scale. In the mining industry, it is mostly handled on an immense scale or at the concentration scale. The difference is, for example, a 20m x 20m x 20m block or within a micrometre scale. Sensor-based sorting is developed in order to explore the mid-scale heterogeneity [10]. Pierre Gy (1978) introduced two terms to classify heterogeneity; constitutional and distributional heterogeneity. These are related to intraparticle and interparticle heterogeneity. Intraparticle is used to describe the uniformity within a particle or rock. Interparticle heterogeneity is used to describe the uniformity between the rocks [10].
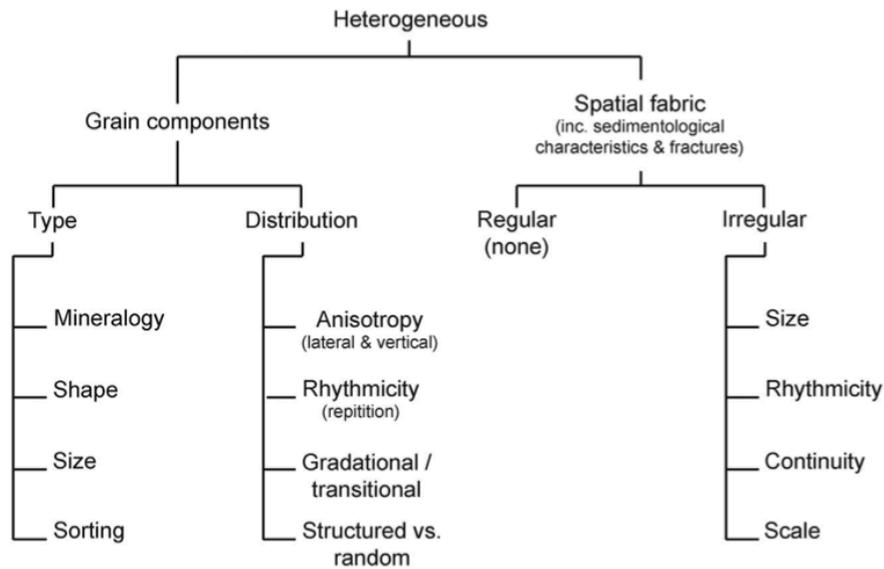
Figure 6. Classification on how heterogeneity can be separated into two 'end-members' of spatial fabric and grain component [11].

To define homo- and heterogeneity, it is necessary to evaluate these terms. Homogeneity is often defined as a compound that is composed of strictly identical fragments. They need to be identical in a complete way; they need to have the same size, composition, density surface morphology, and so on [12]. In a way, it can be said that there are no natural created homogeneous materials or substances. For the sensor-based sorting in the mining industry, it can, therefore, be hard to classify an ore since they are naturally formed and so never can be homogeneous.

The scale is also crucial for assumption in models that can be made to express to the rate of heterogeneity. For example, if a drill core sample (30cm x 5cm x 5cm) will be analysed, how does this relate to a block with the dimension of 20m x 20m x 20m. If it assumed the volume percentage and distribution of the valuable material is the same, the calculation only needs to be converted to a larger volume. This means that if the target element has a grade of 5% in the drill core sample, you will also assume that the grade of the material is 5% in the 20m x 20m x 20m block. Unfortunately, this cannot be assumed for the mineralogy of an unknown material. It is impossible to assume that a surface measurement correlates with such a volume.
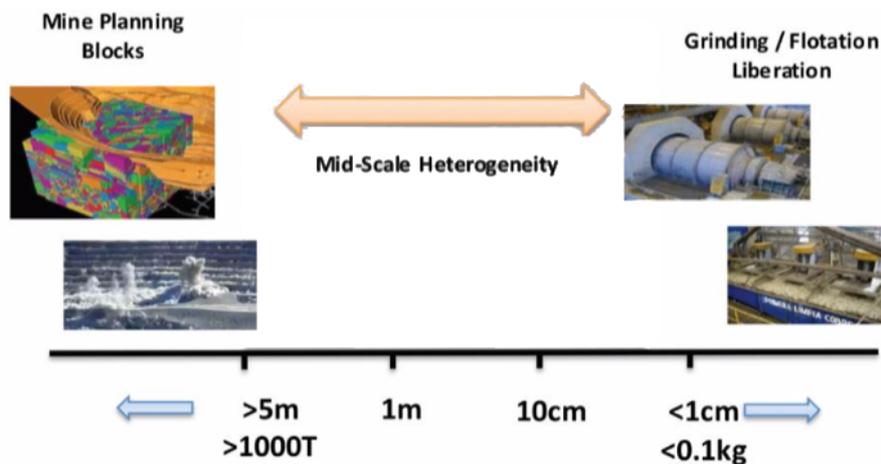
Figure 7. Scaling of mid-scale heterogeneity [10].

If the level of confidence for a small sample is, for example, 95%, it does not imply this is valid for another size or volume. The spatial distribution of elements and mineralization throughout a rock is mostly heterogeneous and can approach homogeneity locally. On the contrary, for large block size, one can see that it approaches homogeneity faster since it has a larger volume which means the variety will be lower than looking on a microscopic scale. A rate of homogeneity is highly dependent on the scale it is evaluated.

4.2 Constitutional heterogeneity

A material is heterogeneous if it consists out of different components. To evaluate a substance analytical, constitutional heterogeneity (CH_L) is used to describe the compositional differences between a set of individual fragments. In the calculation of CH_L, weight factors are introduced. Large fragments have a possibility they differ a lot from the mean, which will indicate the heterogeneity contribution of that part will be more significant. The heterogeneity is assessed so that large fragments will contribute the most to CH_L and small particles will contribute less to the total material heterogeneity [12] [13]. A mathematical summary of the procedure can be found in Appendix A.

To thoroughly analyse an ore, it is necessary to analyse and weigh all constituent fragments. In a rock body of 5m x 5m x 5m, this is possible, but very expensive. Therefore, sampling is needed. The perfect sample can be chosen randomly out of all the loose particles of an ore body. In practice, this cannot happen since there is no access to every free particle. In order to sample, a subset of neighbouring fragment needs to be sufficient. The loose particles can also be seen as a collection of fragments. This introduces a new way of quantifying heterogeneity; distribution heterogeneity (DH_L). Distribution here means distribution in space, distribution within the geometrical volume occupied by the sampling target [12].
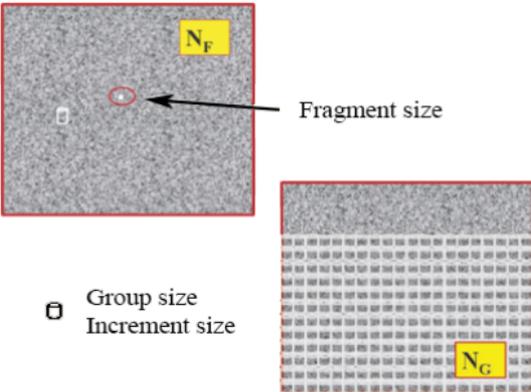
Figure 8. Concept with change from fragment-scale to group-scale; from constitutional to distribution heterogeneity [12].

4.3 Distribution heterogeneity

DH_L is a representation of the differences between groups. Because the entire population of the fragments is available, mixing affects the differences between the groups. With mixing, the groups become more similar, which will result in a higher homogeneity. Mixing will, in the end, result in less variability within the sample. This process is not infinite, at some point, the material has reached the maximal effect of mixing. The heterogeneity will not decrease further.

CH$_L$ evaluates the relation between a single fragment and the group, where DH$_L$ evaluates the heterogeneity between the group and the material sampling target scale, or the size of the lot. Both of the parameters are needed to describe the heterogeneity of any material or substance. CH$_L$ and DH$_L$ are conceptual, theoretical components that in practice always exist intricately interwoven for any material [12]. The differences can be seen graphically in Figure 9.
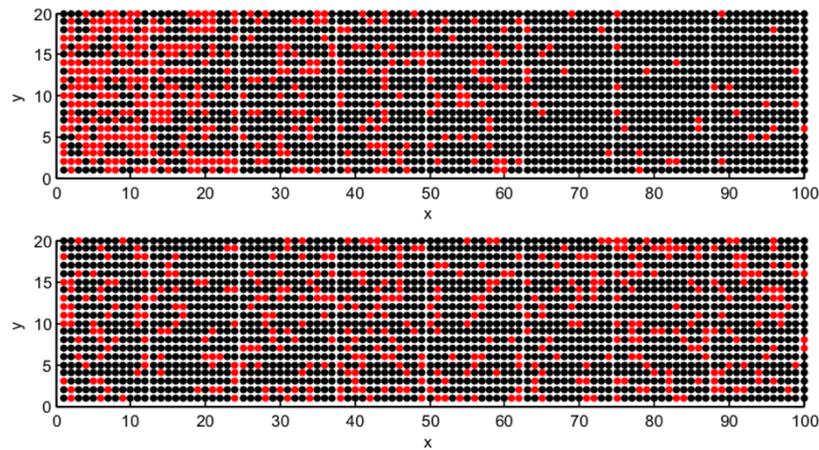
Figure 9. Two lots having the same mean and CH$_L$, but a different DH$_L$ [22].

Two samples have the same CH$_L$; In both images the number of black and red dots are the same. It only looks at points within the image that are the same. If the number of black and red dots vary, the CH$_L$ will be different. It can be seen that the distribution of the black and red dots is different. In the top image, the red dots are more abundant in the left side of the image, where in the bottom image it is more equally distributed.

Using this data for interpreting homo- and heterogeneity within a larger sample will be challenging. Since CH$_L$ and DH$_L$ needs an input which cannot be known from a substance where a composition is unknown. Mandatory parameters are the grade and weight of the total lot, which is impossible to know in both a conveyer setup as with a smaller drill core sample. Defining heterogeneity is possible, but the theory of Pierre Gy cannot be used in order to answer the number of samples needed in order to get a typical answer. It can be used to evaluate and determine heterogeneity but within another context. In the next section, the modelling of heterogeneity will be discussed in order to calculate the minimum sample size.

5. Modelling heterogeneity

5.1 In situ heterogeneity

From a particulate material, with sampling, the variogram and covariance can be calculated. The variogram is a function describing the degree of spatial dependence of a spatial random field. The grains together form, when heterogeneity is assumed, a random structure in 2D, which is not dependent on any direction. For sampling, it would be ideal to have a 0-dimensional target. This target is the only representative if 1) the whole target can be taken as the sample and 2) if the lot to be sampled is mixed before sampling, which can be seen in Figure 11. Evaluating a 0-dimensional target is more comfortable because it can be modelled using a binomial or Poisson distribution function since the material will become more homogeneous and accessible to evaluate analytically. This is used in the theory discussed above, where constitution and distribution heterogeneity are mentioned.
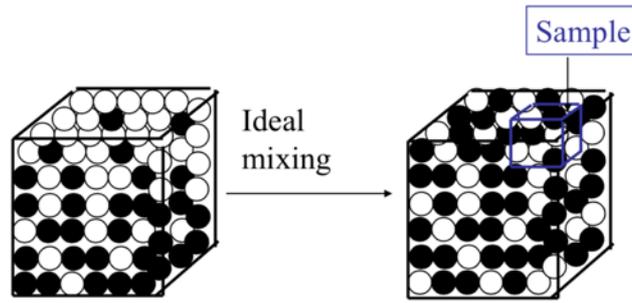
Figure 10. Principle of mixing for a 0-dimensional sampling target [22].

When a theoretical sample is made, true point samples can be taken in order to evaluate the heterogeneity. This means that a x by y grid is created and the volume fraction of interest is known, so that can be said that, for example, 70% is element A, 20% is element B and 10% is element C. In this case, if one samples n points with known areal fraction (f), it is expected that that the number of hits on the area of interest is equal to $\bar{x} = n * f$. With this information known, the variance can be calculated; $var\{x\} = nf(1 - f)$. This can be summarized, for point samples, into the formula below. If the grade of the area of interest will decrease, the variance of sampling will increase. Here, the variance for a random point sample is found with n = 1, and the sill (section 5.2) of the variogram must be equal to $f(1 - f)$ [14]

$$\frac{var\{x\}}{\bar{x}^2} = \frac{nf(1 - f)}{(nf)^2} = \frac{1 - f}{nf}$$

5.2 Geostatistics

For describing the variance within in mineral materials, geostatistics can be used in order to predict values in a mesh grid, given an amount of sample point measurements. Geostatistics describes a domain with a random function [15]. Evaluating a limited number of samples gives more boundary conditions since the volume is not as large as infinity. One can define certain boundary conditions at one sight. For example, within a drill core of 50 centimetres, it is easier to define boundary conditions than for an 8000 m³ block.

For analytical purposes it is easier to model a finite sample, since the total surface or volume is known. This can be used for the analysis of the sampling values compared with the lot. When describing the distribution of elements within a lot, a variogram is often used. This is a function taking a definite value in each point of space. It describes a curve which represents the degree of continuity of the mineralization [16]. It was first defined by Matheron (1963):

$$\gamma(h) = \frac{1}{2V} \iiint_V [f(M + h) - f(M)]^2 dV$$

Here, M is a point in the field V, and f(M) is the value at that point. One of the most important parameters is h; the separation or lag distance of interest. To create the semivariogram for a given $\gamma(h)$, all pairs of points at that exact distance would be sampled. Unfortunately, in practice, it is impossible to sample everywhere so that an experimental variogram will be created based on the values obtained with the function given above.

To create the final variogram, in general, three steps are needed. First, based on the known sample points and their corresponding values, the experimental variogram is calculated. Next, a variogram is tried to be fitted within the points created in the previous steps. The most important parameters here are initial values for the range and the sill. The range represents the distance limit beyond which the data is no longer correlated over distance. The sill represents the variance of the variable. Finally, the definitive variogram will be fitted with the variogram and can be used in practices like kriging.

However, the formula described above is valid for a volume, which is three-dimensional. For analysis with LIBS, a 2D image of a sample is measured and used to evaluate the lot. Therefore, this formula can be simplified into the following expression:

$$\gamma(h) = \frac{1}{2N(h)} \sum_{i=1}^{N(h)} (z_{xi} - z_{xi+h})^2$$

Here, z_x is the known value at the location x, z_{x+h} is the known value at a distance h from the point z_x. N(h) is the total number of combinations within the distance h. As mentioned above, the sill, range and nugget are the most important parameters for describing a (semi)variogram. An example, including the parameters, is shown in Figure 11.

The range and sill correspond to the distance where the data is no longer correlated over distance. The sill is the maximum value for the value of the variogram and the range the distance at which this will occur. The nugget effect is a small-scale variation or an error within the measurements. If a nugget effect is there, the variogram model will be "lifted" upwards to create an intersection with the y-axis which is not equal to zero. Linking this to the sample size, it is assumed that the smaller the range, the more heterogeneity, which will require more samples.
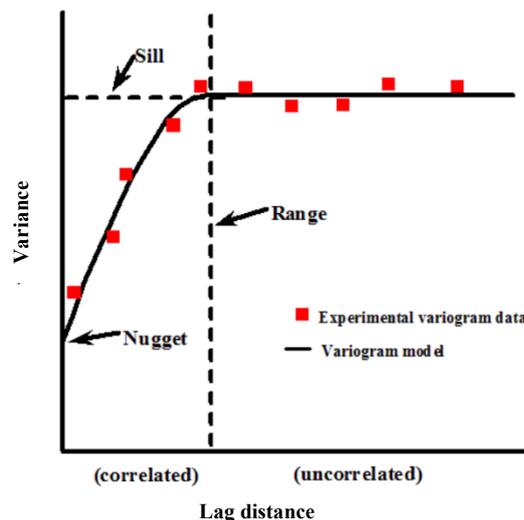
Figure 11. Example of a fitted variogram with the sill, range and nugget effect [23].

When sampling in 2D, it is crucial to select the right sample size. It is generally known that as the size of a sample increases, the sampling variance decreases because it is evaluated over a greater area. Lyman (2011) composed two theoretical case studies in order to determine the relationship between variance and sampling size within a theoretical situation.

In the first case, a sample is composed of three phases; black, grey and the white background. This texture is based on a Boolean random set oriented with a size distribution of 5 to 100 pixels on edge with a 90% passing size of 70 pixels. The black and grey fractions have a proportion of 35%, which leaves a fraction of 30% for the white background. It is mentioned that this texture is typical for an ore containing relatively large grains of pyrite [14].
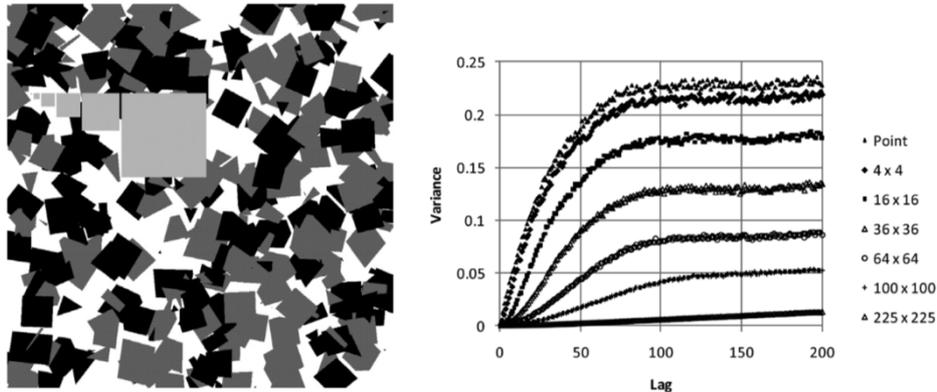
Figure 12. A texture of cubic grains at 35%. volume fraction, modelled phases are highlighted. Right; the variograms of the corresponding sample sizes are shown [14].

The variogram in Figure 12 is calculated focused on the black phase using 10000 random points for a series of sample sizes. The theory mentioned above is said to be true since the sill decreases when the range of the variogram increases. In LIBS analysis, the variogram of the rock sample, for example, a drill core, can be used in order to estimate the average size of the phases of interest, and also how the resolution of the variogram decreases while the sampling area will be increased.

The other case study is carried out for material with multiple nuggets. The paper states that the target phase has an aerial fraction of only 1.62% [14], this is much lower than 35% before.
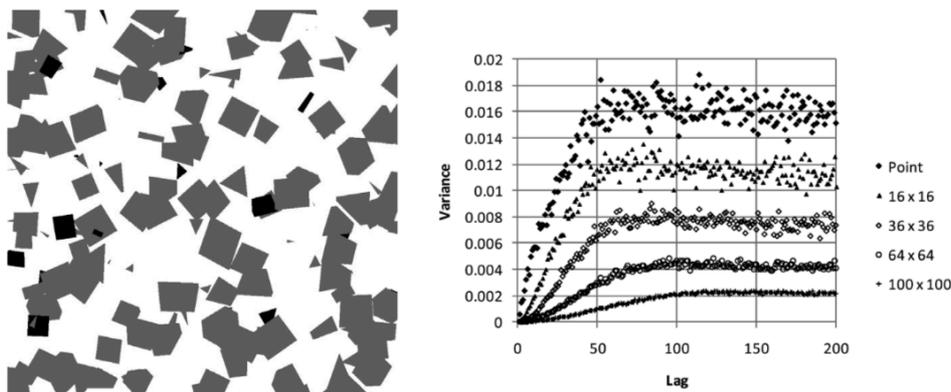
Figure 13. A texture with higher nugget effect, cubic grains only 1.62%. Right; the variograms of the corresponding sample sizes are shown [14].

Figure 13 only contains a few fragments of the target phase. One would expect that the results for the variogram would be different, which can also be seen. Comparing both variograms, one can say that they are similar, but the values for the variance vary. Only the sample size of 225x225 pixels is not used in the second case study.

For analysing heterogeneity, Lyman et al. (2011) shows that a mineral texture has an associated variogram which characterizes its spatial covariance. Here, the direction of measurements is essential. The study gives a glaring example of a banded structure where the variogram in the direction typical to the bands will show a periodic structure. In the other direction, the variogram would look very different [14].

The study offers two possibilities for a measure of heterogeneity; the best possibility is the range of the corresponding variogram. To add an extra measurement, the sill can also be considered. Comparing two materials with a known sill variance, it can be assumed that the one with the shorter range would be more heterogeneous than the other. This indicates it would need more samples to reduce the estimation variance for a given block size [14].

The study concludes that when an orebody is sampled on a microscopic level, the variogram should not show a nugget intercept even when the target phase is highly discontinuous, which is equal to a so called "nugget-effect." The downside is that for each analyte, the measurements will be different which will result in different results for the variogram. In the end, apart from special cases of diamonds and gold, there is no reasonable link between in situ heterogeneity and particulate heterogeneity, which would make it hard to link surface measurements to the in-situ composition of the material.

It is important to mention that for successful characterization of the material using geostatistics, it is necessary to prepare the ore. This involves several stages of breakage and mass reduction which can reduce the speed to characterize a sample since beneficiation takes more time then real-time measurements.

5.3 Statistics

Basic statistics can be used to evaluate the precision of a particular sample size. This can be done using the mean and the standard deviation for different sample sizes. As mentioned, the standard deviation is assumed to decrease with increasing sample size. In later sections, this will be evaluated. The standard deviation and mean of a sample are calculated follows:

$$SD_{sample} = \sqrt{\frac{\sum |x - \overline{x}|^2}{n - 1}}, \qquad Mean_{sample} = \frac{\sum x}{n},$$

The formula for calculating the standard deviation of a sample is different to calculating the standard deviation for a whole population. For example, the numerator is *n - 1* where for a whole population it is equal to just *n* [17]. From section 6.2, these formulas will be used in order to evaluate the levels of certainty for different sample sizes for a 50x50 pixel^2 grid.

5.4 Image analysis

Evaluating heterogeneity could be done using image analysis. In combination with libs, one could combine these principles to assess heterogeneity per shot taken. Some papers are published on automatic heterogeneity determination using images. This paragraph will evaluate the potential of this technique. De Moura França et al. (2017) created a tool for evaluated homogeneity for images using a homogeneity curve. It based on the continuous-level moving block method (CLMB), which is relying on consecutive sub-sampling of one image in sub-sample window of different sizes.

First a picture divided into sections, where after the standard deviation is calculated based on the size of the sampled fraction. Figure 14 gives an overview of the working principle. The picture is evaluated for all sub-windows $(I' \times J')$ possible within the whole sample $(I \times J)$. The size of the sub-window can be formulated as $PIX_{S_{I'J'}} = I' \times J'$. The total number of sub-samples for all sub-window van be calculated as follows:

$$TOTAL_{S_{I'J'}} = [I - (I' - 1)] * [J - (J' - 1)]$$
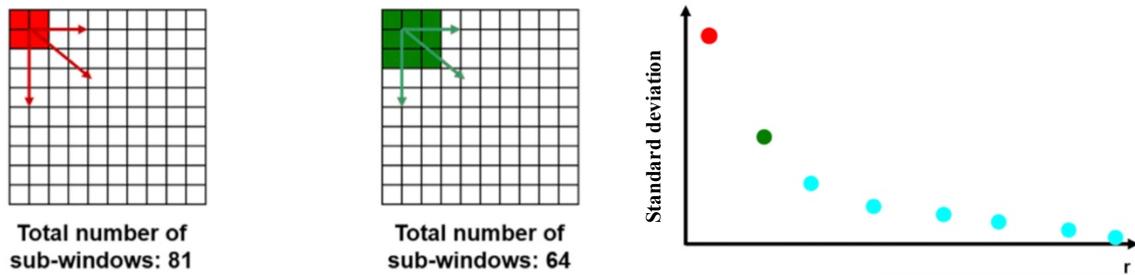
Figure 14. Left and middle; two examples of sub-windows with a size of two and three squared pixels. On the right, the corresponding value of the mean standard deviation of all the sub-windows [24].

Afterwards, the standard deviation for all sub-samples is calculated and the sum of these values will be used to calculate the standard deviation for each sub-sample windows size which is available. These values are used for the vertical axis. For the horizontal axis is scalar is used, named r and is defined as $r = (I' \times J')/(I \times J)$. It is expected that with an increasing sub-sample size, the standard deviation will decrease. How steeper the graph will be, the more homogeneous the sample is. The homogeneity curve is made by first calculating the standard deviation ($SD_{I' \times J'}$), for all possible locations of the sub samples, then the sum of the standard deviations is divided by the total number of sub-samples (SD_{plot}). SD_{plot} is plotted against r.

$$SD_{I' \times J'} = \sqrt{\frac{\sum_{I'=1}^{I'} \sum_{J'=1}^{J'} \left(TOTAL_{S_{I'J'}} - \bar{s}\right)^2}{PIX_{S_{I'J'}} - 1}}$$

$$SD_{plot} = \frac{\sum SD_{I' \times J'}}{TOTAL_{S_{I'J'}}}$$

Figure 15 shows three theoretical situations where the homogeneity curve can be observed. All images have a white colour area of three percent, but these pixels are different looking at their distribution. The minimum size is one squared pixel. First, three nuggets (10 pixel^2) within the sample are evaluated, followed by five and one pixel^2 variants. It can be seen that the homogeneity curve behaves different looking at samples A, B and C. As said before, the line will approach a standard deviation of zero faster when the sample is more homogeneous.

For LIBS, in section 6.2, the model will be evaluated and tested and evaluated for different homo- and heterogeneous samples; theoretical and real-life.
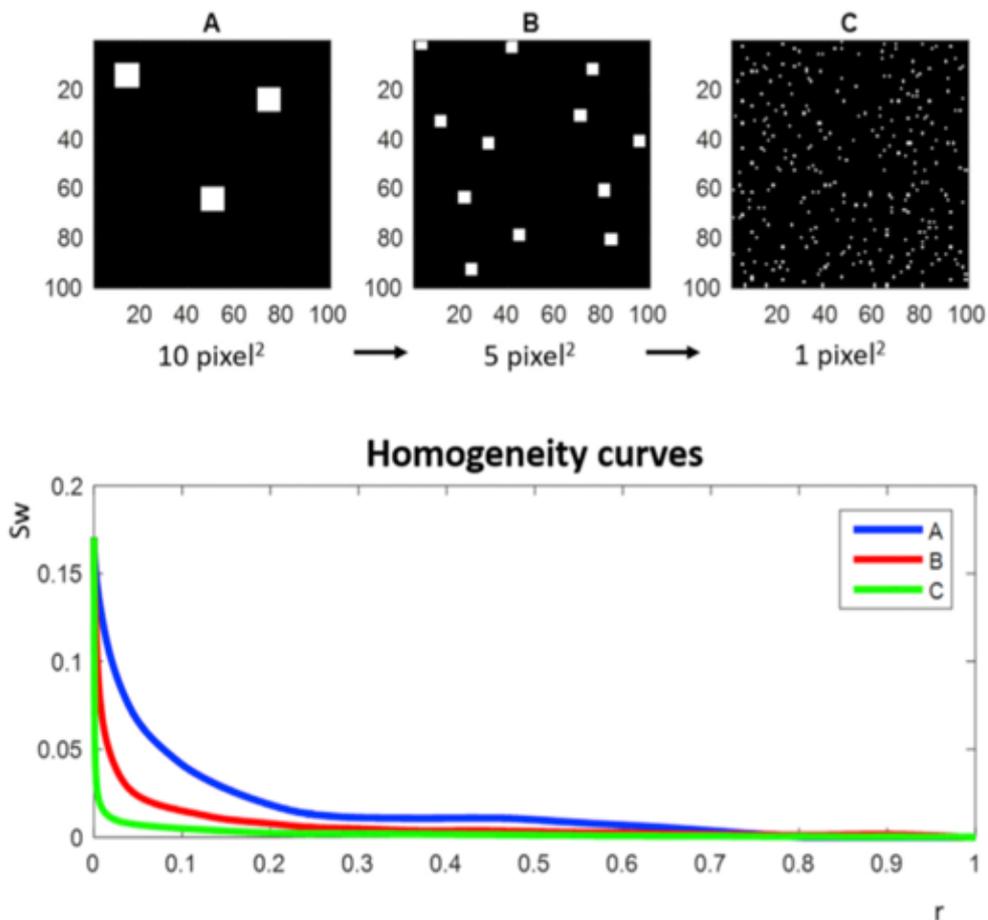
Figure 15. Simulation of a case in which the concentration of white pixels is the same in the three images, but the distribution differs [24].

Using the homogeneity curve give a solution to defining the homogeneity of a mono-channel image. It can be used to evaluate the homogeneity of images containing a minimum og two elements. For LIBS characterisation, this can be useful to evaluate the minimum required sample size. Chapter 6 investigates the homogeneity curve more in depth for relevant case studies. One of the case studies investigates the homogeneity percentage, obtained with the homogeneity curve, with the minimum sample size to be within a certain margin of error. As it is expected that this will correlate.

6. Case studies

6.1 First impression: LIBS for tailing slurries

As mentioned before, it is expected that with an increasing number of samples, the standard error will decrease. A simple test case is created to evaluate if this is true. Therefore, a mineralogical assay is used of the tailing samples measured by the paper of Khajehzadeh et al. (2016). The mineralogic information was provided by the Mineral Liberation Analyzer (MLA) method. They consist out of fourteen samples from a tailing stream slurry in a flotation plant, which belongs to an iron ore concentrator. It is assumed that a composition of a slurry is relatively homogeneous, which means the composition are assumed to be the same.

In order to provide a reliable answer and compensate instabilities and reduce the noise, three LIBS spectra per sample were measured. Each spectrum covered a wavelength range from 190nm to 507nm and was the result of 200 accumulated laser pulses. For the three measurements taken, the average was noted. The complete assay can be found in Appendix B.

For evaluating the use of more samples, the standard deviation (SD or σ), the standard error of the mean (SEM) and the coefficient of variation (CV) for increasing sample size are calculated. This means the data is evaluated for 1, 2, 3, …, 14 samples;

$$SD = \sqrt{\frac{\sum |x - \mu|^2}{n - 1}}, \qquad SEM = \frac{SD}{\sqrt{n}}, \qquad CV = \frac{SD}{mean}$$

Figure 16 gives an overview of the results for an increasing sample size. The standard deviation of the data increases rapidly for the circa the first five measurements but becomes more constant afterward. This indicates the data is becoming more stable with less variation. A more stable σ will result in a lower SEM since the number of samples (n) increases while σ stays relatively constant. The CV is the ratio between SD and the mean. In the plot is shown that up to five samples the CV increases, where after fluctuates. It can be said that an increasing sample size contributes positively to the material characterization.
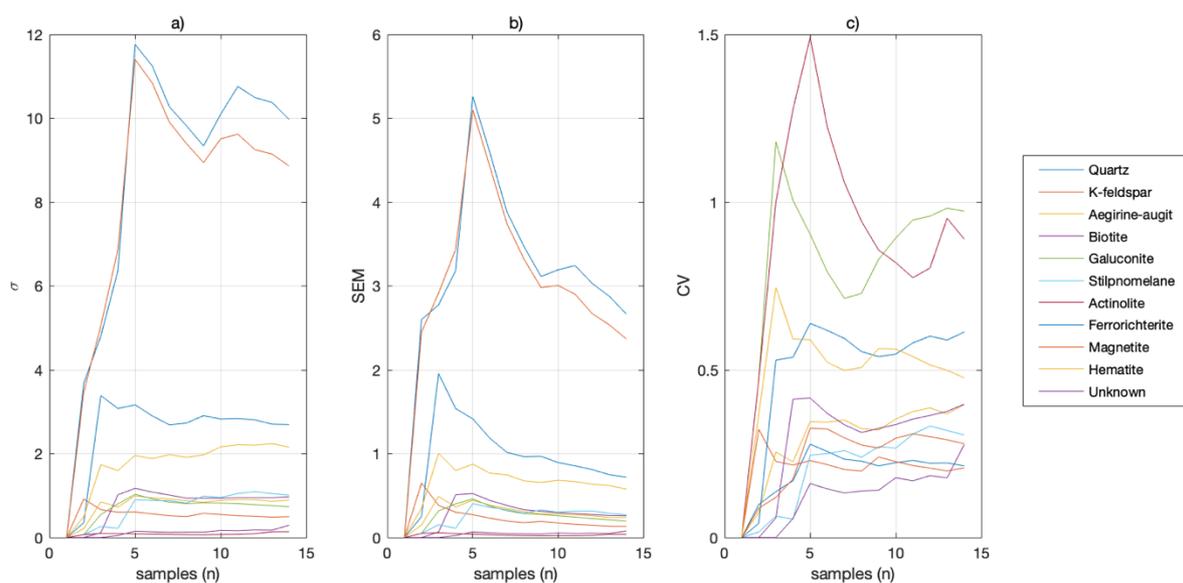
Figure 16. a) Standard deviation (σ), b) standard error of the mean (SEM) and c) the coefficient of variation (CV) for the data of element tailings characterization using LIBS [4].

6.2 Theoretically generated images

Evaluating the sample size is difficult to achieve with real examples since the overall composition is not known. Therefore, it is hard to calculate how the results of the sample measurements compare with the overall material. With LIBS, it is possible to create images as Figure 17. Analysing this picture could indicate the grade of the sample, but it is not known what the total composition is. In order to do so, a theoretical model needs to be created where the overall composition can be determined. From that created material, random samples need to be taken in order compare how many samples are needed in order to give a sufficient estimation of the total material.
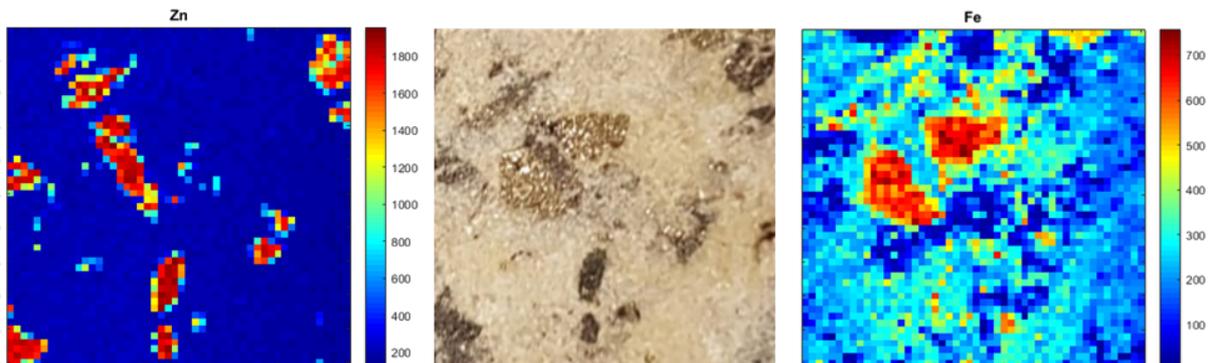
Figure 17. LIBS characterization results for Zn and Fe for a sample measurement [28].

A 50 pixel^2 grid is created. For this grid, the grade percentages of a particular component can be inserted to create an image similar to Figure 17, which is created with 2500 LIBS spots. The pixels are divided for the assigned grade values and randomly distributed using the `Sample` and `Shuffle` functions in MATLAB, created by Daniel T. Kaplan [18]. The sample sizes will be evaluated for three cases, where the composition differs and increases;

Case 1:	**Case 2:**	**Case 3:**
40%, 30% and 30%	70%, 15%, 10% and 5%	97%, 2% and 1%
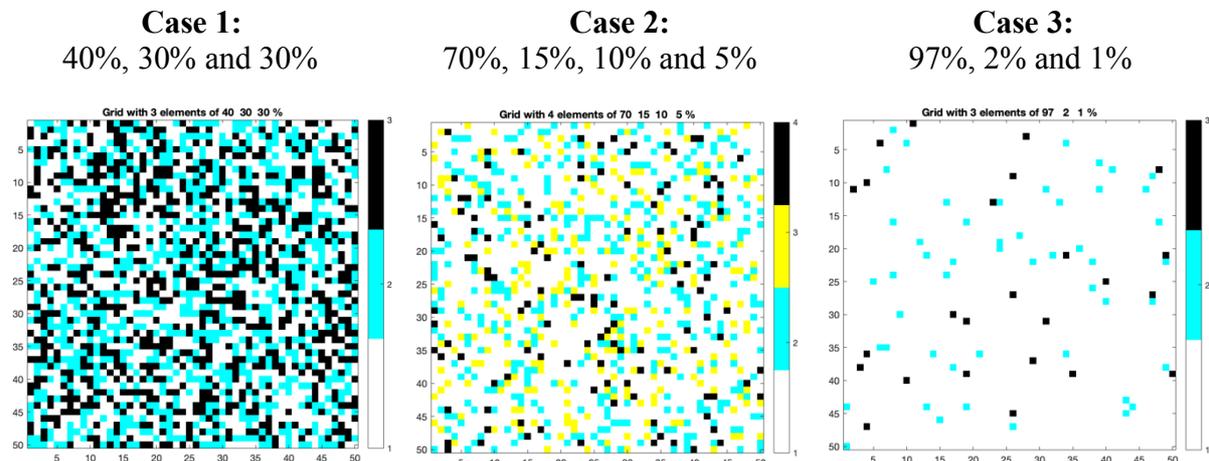
For Case 2 a general composition is chosen, a typical distribution of pyrite also used in section 0. Case 2 involves a distribution containing four elements with one significant contributor. The remaining are 15%, 10% and 5%. Case 3 consist almost out of one element (97%), with two other elements contributing only 1% and 2%. It has to be noted that the examples given above are one representation of a possibility. For each run, another sample will be created to increase the randomness of the model.

For calculations, it is assumed that the spot size for LIBS measurements is 600x600µm2. This indicates for a 50x50-pixel grid, and the dimensions are 3x3cm. The theoretical cases are based upon these dimensions. It is assumed that the standard deviation will decrease with an increasing number of samples and the mean of the sample will approach the mean of the lot. For the three cases above, the standard deviation is calculated numerical from one until 2500 samples. For each sample size, 1000 different samples are taken. For each sample, the grade is calculated. For these 1000 grades per sample size, the mean and standard deviation is calculated and plotted. The results for Case 1 can be seen below. The results for Case 2 and Case 3 can be found in Appendix E in Figure 36 and Figure 37.

It needs to be mentioned that the x-axis is shown in a percentage of the total population (=2500 pixels) and the y-axis shows the absolute percentage, so not a proportion of the true grade shown with the red dotted line.
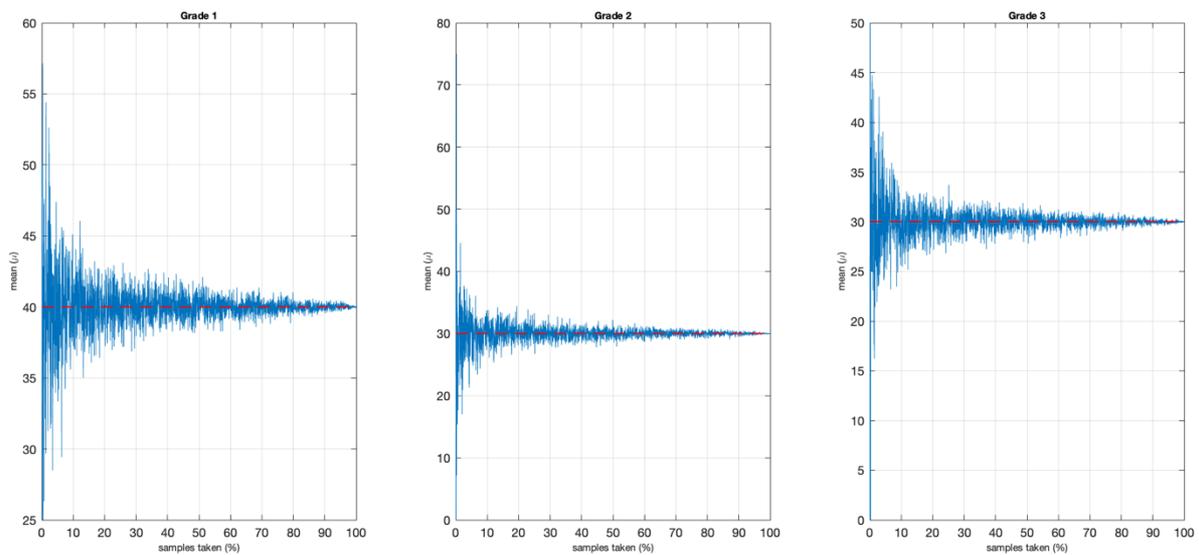
Figure 18. Results of the mean for Case 1 (40%, 30% and 30%), for an increasing sample size.
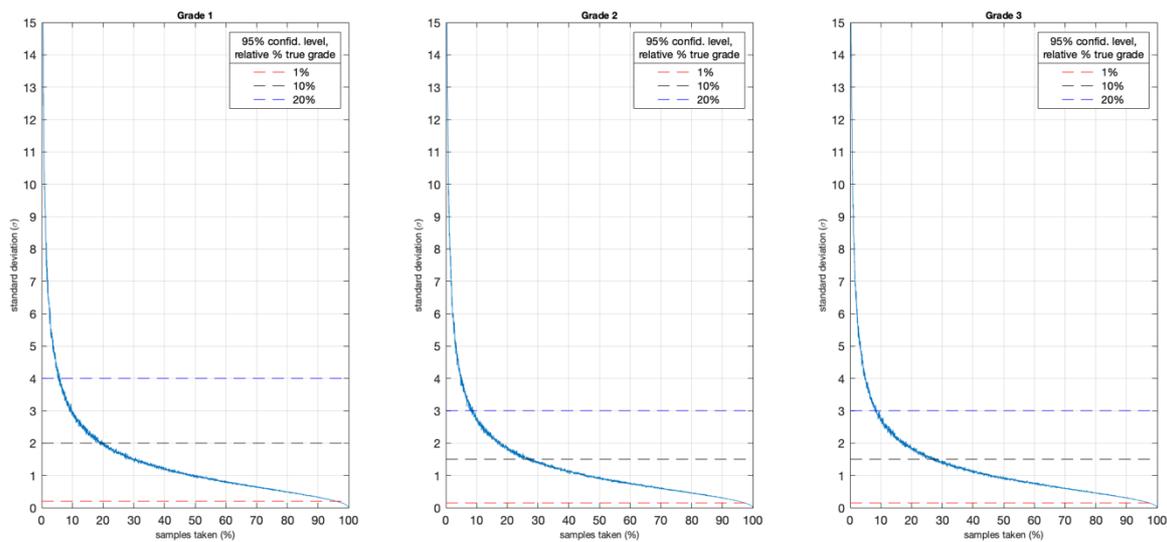
Figure 19. Results of the standard deviation for Case 1 (40%, 30% and 30%), for an increasing sample size.

19

For a maximum of 2500 samples, it is observed that both the mean and the standard deviation decrease over an increasing sample size. According to Cochran, for a population of 2500 (50x50) with a margin of error of 5% and a level of confidence of 95%, the recommended sample size is equal to 333 (=±14%). Comparing this with Figure 18 and Figure 19, the mean varies between absolute ±5% from the true mean. For a relative more accurate percentage, the sample size will be higher. If a higher level of confidence is desired, the standard deviation is required to be lower. For a standard deviation of 2%, a minimum sample size of 1500 is required. The standard deviation and confidence level are linked to each other, where one standard deviation from the mean is equal to 68% confidence level, two standard deviations from the mean is equal to 95% confidence level and three standard deviations from the mean is equal to 95% confidence level.

To calculate the percentage of homogeneity, the image analysis tool by De Moura França et al. (2017) is used. First, this is done for the original image, then the material is converted into a homogeneous form. Last, it is converted to a heterogeneous material. Furthermore, the histogram of the original picture is shown. For all the original, the homogeneous and the heterogeneous case, the homogeneity curves are plotted. Comparing the line of the original material with the homo- and heterogeneous curves, a percentage can be assumed.

For Case 1, it can be seen that the original input versus the homogeneous case is not very different. They are almost similar, only their distribution varies. The differences between the original input versus the heterogeneous case are apparent. Since there are no differences between the original and the homogeneous case, the percentage of homogeneity is assumed to be 100%. Because the original image is generated randomly with the input parameters for the grade distribution, the pixels are also distributed randomly. This, in the end, generates a homogenous material looking at the spatial distribution. To evaluate this further, more heterogeneous samples need to be researched.
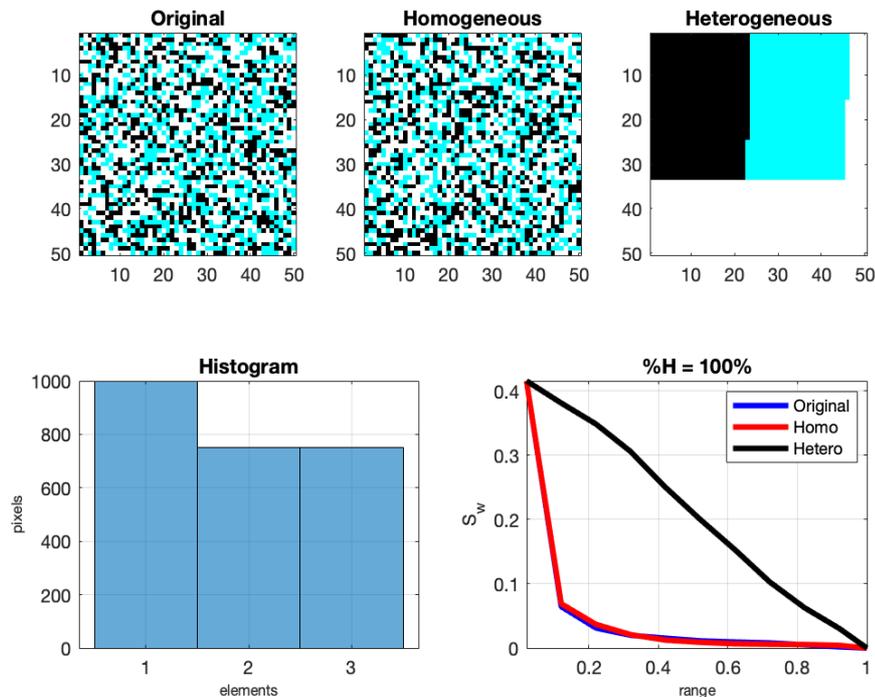
Figure 20. Top: overview of the original, (theoretical) homo- and heterogeneous material. Bottom: histogram of the distribution and the homogeneity curves of the images above. Also, the homogeneity percentage is displayed.

For Cases 1, 2 and 3 on page 18, the homogeneity percentages are evaluated at respectively 100%, 98%, and 97%. In Appendix E; Figure 37, it can be seen that in the case of a low-grade image (Case 3), the grades converge to their given grades of 97%, 2%, and 1%. However, for estimating the grade of 2% and 1%, the standard deviations are well above 2% until 1000 samples are taken. For example, assessing the grade this indicates a grade of 3% or -1%, which is impossible. To have a confidence level of 95%, two standard deviations are needed (Figure 5). To be within 0.2% of the true known grade, a minimum of 2000 samples is needed within the population size of 2500.

If the sample has a grade of 40%, 30%, and 30% and is evenly distributed, the sample size for characterization is relatively low since the composition is close to 1/3 of each element. Therefore, two general cases are evaluated for a vein and a nugget structure in order to evaluate differences in the homogeneity percentage, the mean and the standard deviation.
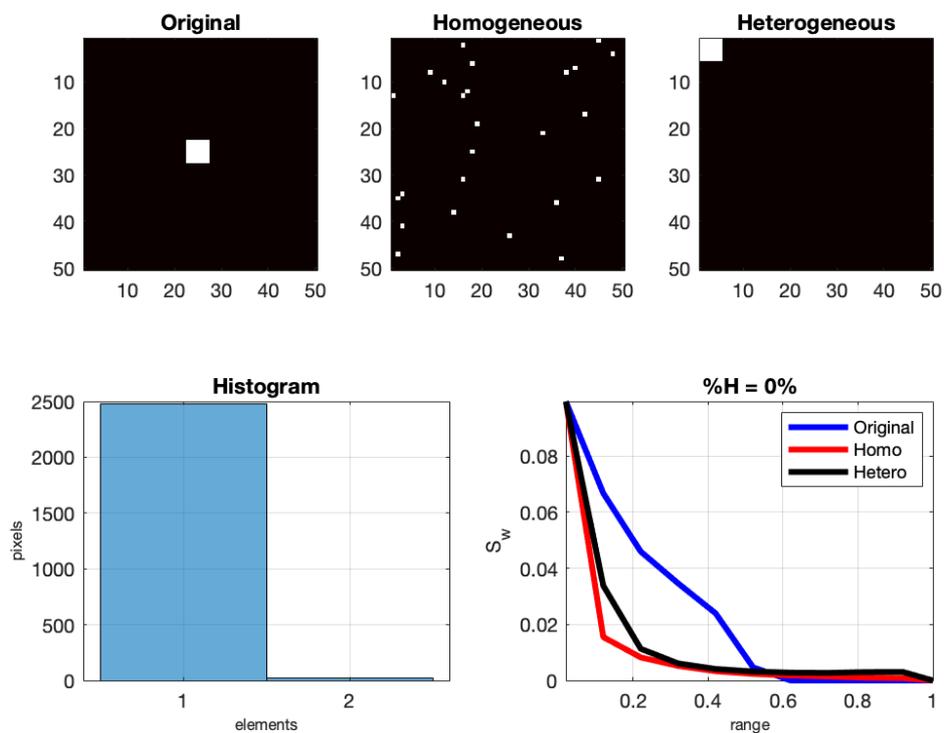
Figure 21. Theoretical case for a "nuggety" structure with grade distribution of 99% and 1%.

Figure 21 shows the homogeneity curves for the images above. The homogeneity percentage is 0% and is calculated with the image analysis tool mentioned in section 5.4. This indicates a heterogeneous distribution what can be expected with a nugget in the centre of the image. The areal percentage of black pixels is 99%, and the white "nugget" contributes 1% to the total.

Figure 23 and Figure 22 show the mean and standard deviation of Figure 21. Due to the low concentration of the nugget, for relative sample sizes below 10%, it is still possible to determine the sample as 100% pure (no nugget). Afterward, the mean converges more to the known grade of 99%. It indicates how hard it is to determine the grade of a sample with a limited number of samples taken. Looking at the standard deviation, a minimum of 80% samples are needed to have a confidence interval of 95% to be within 0.5% precision of the measured mean. This is very high compared to the total image size of 2500 pixels. It indicates that with a "nuggety" image, the sample size needs to be extremely high to detect those low-available elements.
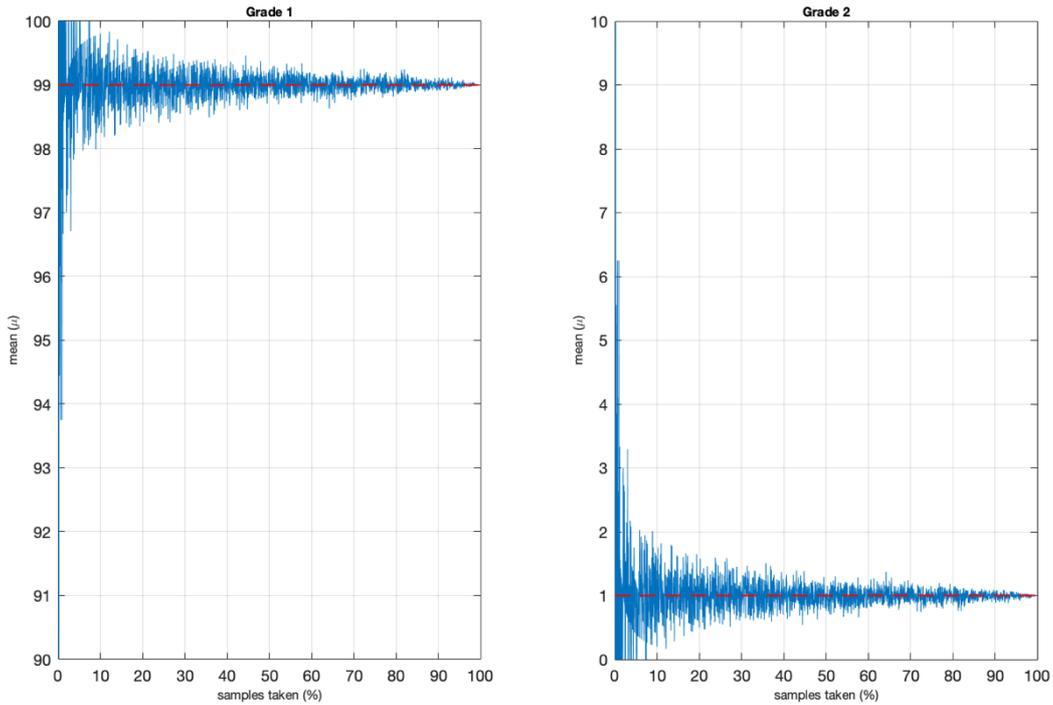
Figure 23. Mean of the "nuggety" structure versus the sample size.
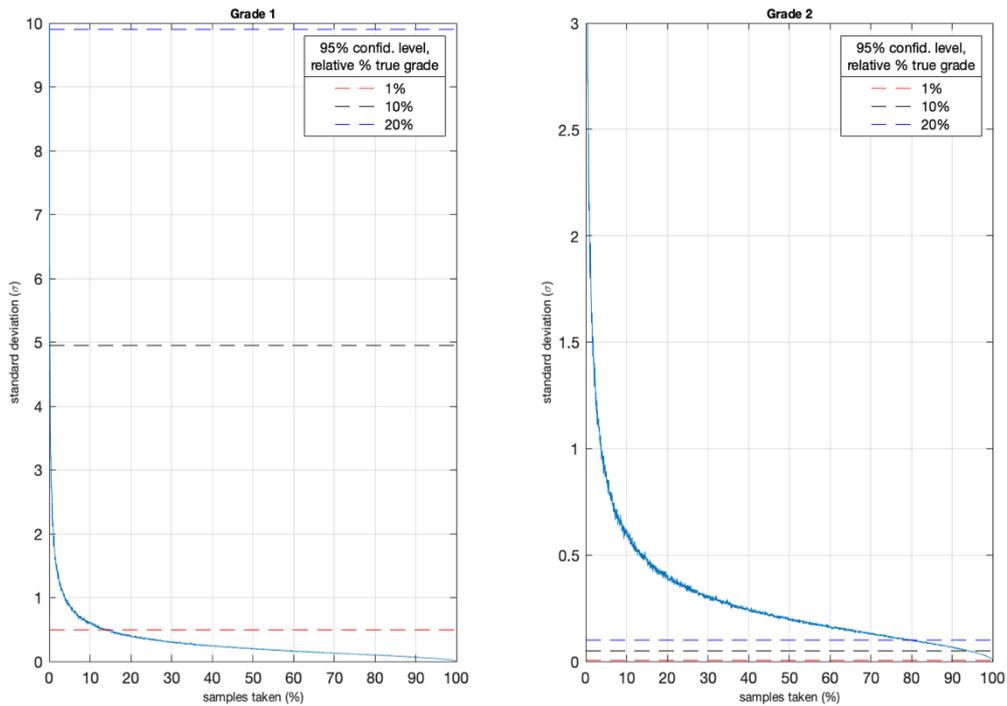
Figure 22. Standard deviation of the "nuggety" structure versus the sample size.

The same is done for the "vein" structure, where on a band of secondary material is evaluated. This has resulted in a grade distribution of 88% and 12%. As can be seen in Figure 24, the homogeneity percentage is evaluated to be 10%, which is still low but higher than the case of the "nuggety" texture. The standard deviations of the "nugget" texture are lower, but compared to the known true grade the differences are more extensive. The standard deviation shows absolute percentages, which indicates most of the values are below 1%. This would indicate characterization between 0% and 2%, what is not accuracy on such a small scale.
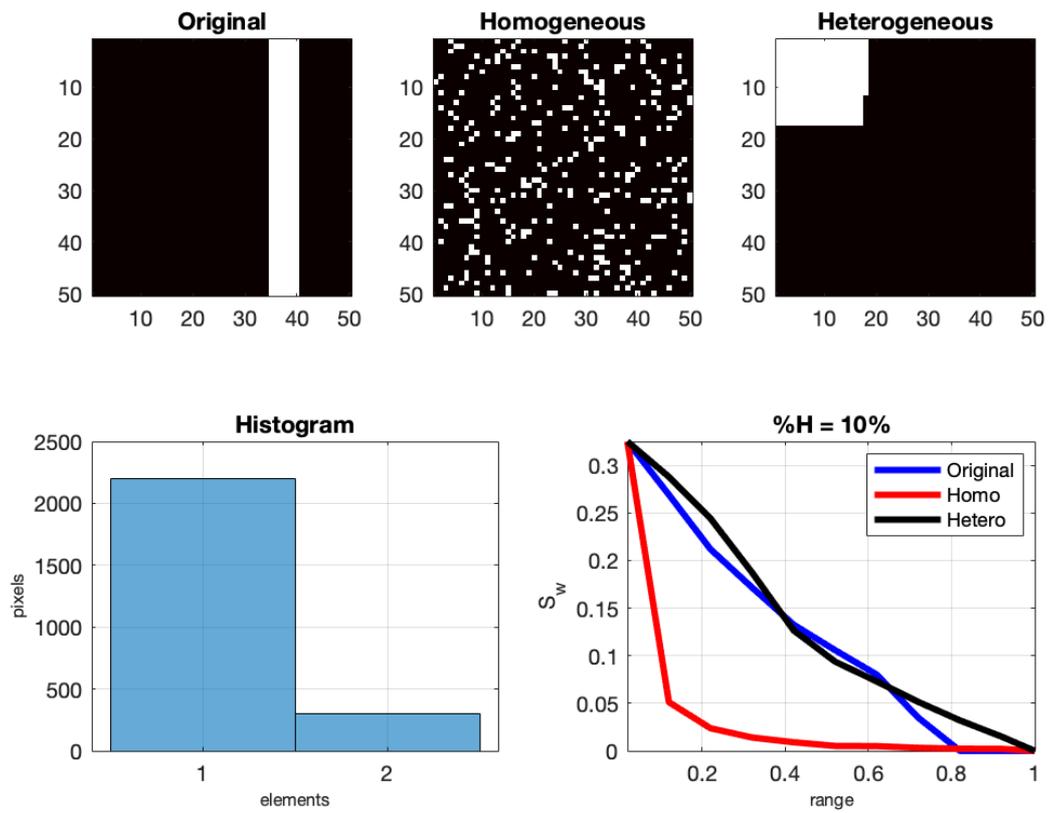
Figure 24. Theoretical case for a "vein" structure with grade distribution of 88% and 12%.
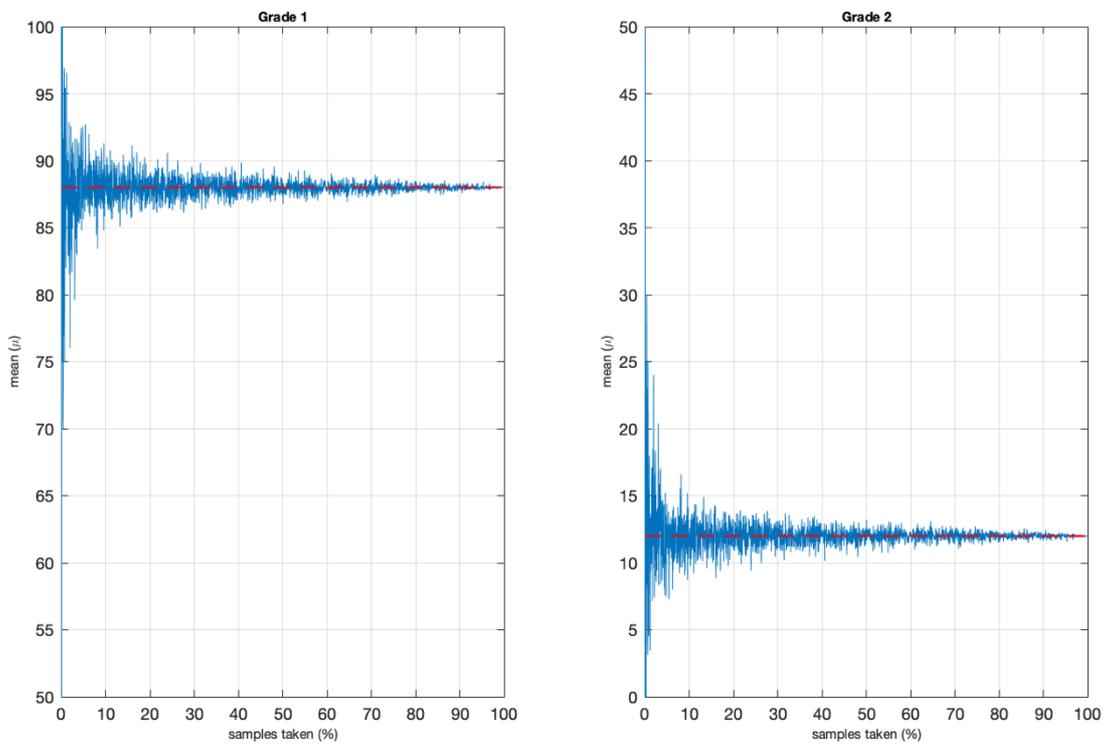
Figure 25. Mean of the "vein" structure versus the sample size.
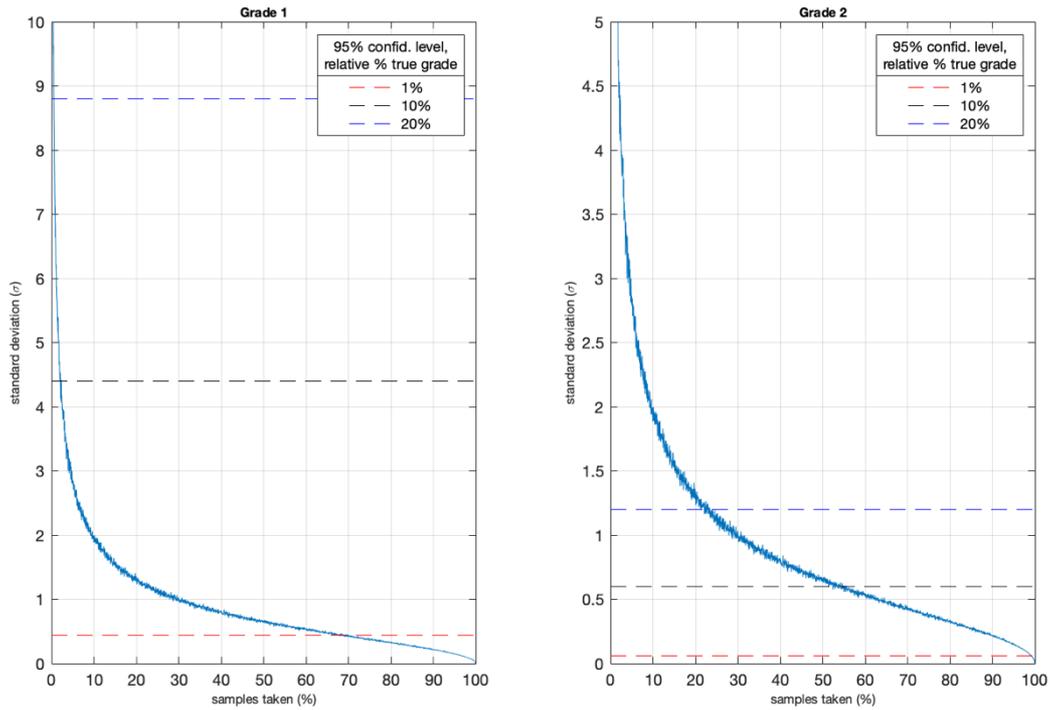
Figure 26. Standard deviation of the "vein" structure versus the sample size.

Figure 25 shown that the variances of the mean for the vein structure vary less than for the nugget texture. This can be explained due to the relative higher concentration of the two elements (88/12% vs. 99/1%). Due to the grades of 88% and 12%, the standard deviation in Figure 26 drops later below 1 than the nugget structure. Also, this can be explained due to the higher target grades within the image.

When two elements are evaluated, the standard deviations for both elements are similar, due to the factor that their differences will be the same. If the selected grade of a sample for one is 90%, the other is equal to 10%. Moreover, another run results in 80% and 20%. For both elements, the standard deviations will be 5%. With a more significant number of elements, the standard deviations will vary per elements, since it is not the case that if the grade x is known, the other grade is equal to $100 - x$.

With a small number of samples, in Figure 23 and Figure 25 it can be seen that the mean of the image fluctuates a lot. For a true grade of 88%, with a sample size of 20%, the measured grade can still be 91% or 85%. For determining the number of samples needed for sufficient characterization, the grade distribution, some elements, and the spatial distribution is essential. Changes within these parameters result in another standard deviation of the true grade. From the graphs of the standard deviations, one can calculate the sample size to within 1% of the true grade for different confidence levels. Most likely these are 68%, 95%, and 99% since they are equal to one, two and three standard deviations, see also Figure 5.

In this section, theoretically generated images were used in order to calculate the homogeneity percentage, the mean and standard deviations for their corresponding sample sizes within a 50x50 pixel2 grid, where they will be compared. Standard deviations are now evaluated for homogeneity percentages of 100%, 98%, 97%, 0% and 10%. In the next section, other percentages of homogeneity will be discussed, in order to evaluate images from 0% to 100% of homogeneity. These images are based upon real-life rock images, like chalk and granite.

6.3 Real-sample based images

As mentioned above, it is hard to generate randomly distribute a certain grade distribution, since the pixels will always be distribution in homogeneous way. Therefore, other images are created based upon real rocks images. This is done to reduce the level of homogeneity within the images and increase the variety of the generated homogeneity percentages. The images used are samples of gneiss, chalk, granite and peridotite. The jpg images are loaded into MATLAB with `imread`, where after they are converted to a mono-channel image with help of the `rgb2ind` function. They the matrix a conversion to a 50x50 pixel^2 grid using `imresize`. The last step is a conversion to a double array using `im2double`. Below these transformations are shown. It has to be mentioned that the accuracy will be decreased.
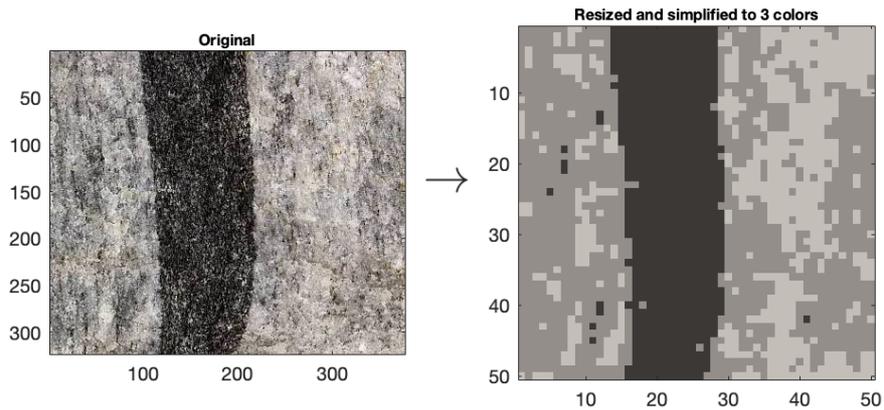
Figure 29. Mono-channel image generated based on a gneiss rock sample. %H = 29%
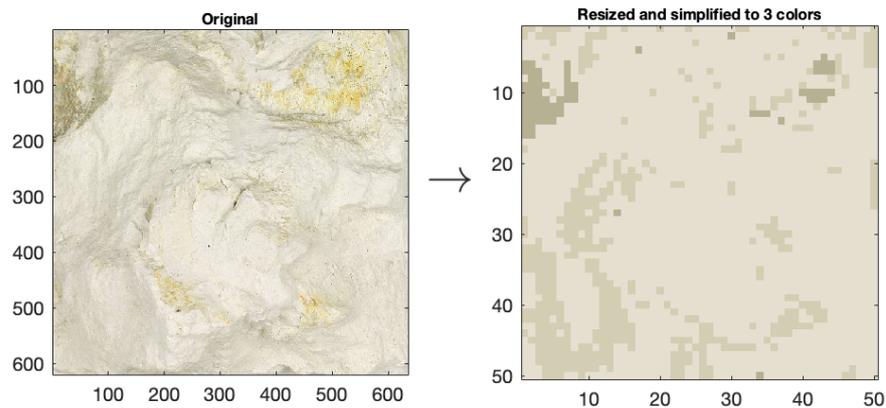
Figure 28. Mono-channel image generated based on a chalk rock sample. %H = 55%.
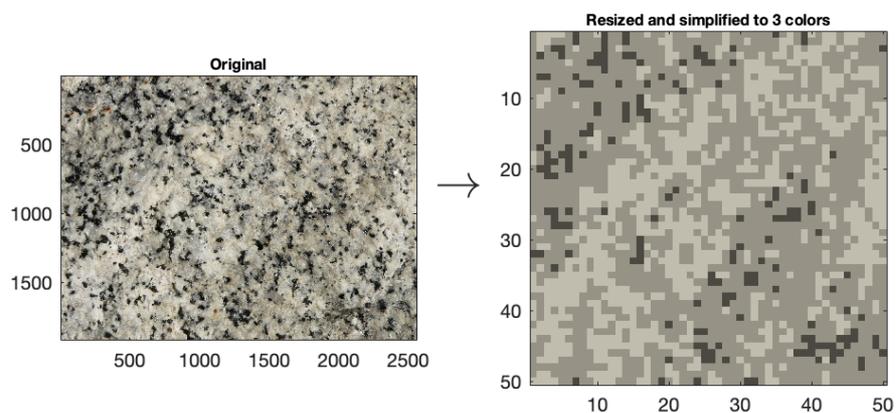
Figure 27. Mono-channel image generated based on a granite rock sample. %H = 71%
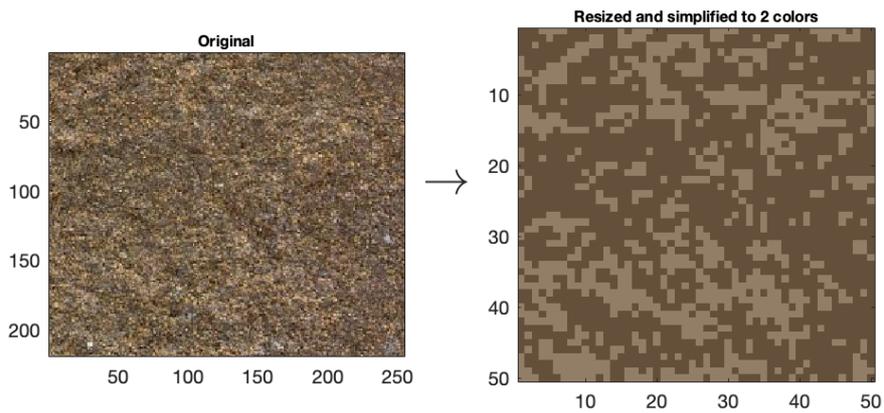
Figure 30. Mono-channel image generated based on a peridotite rock sample. %H = 85%

For these images, 1 - 2500 samples are taken. This is done 1000 times per sample size, and the standard deviations are calculated over these 1000 measurements. The mean is calculated only for two samples since this will increase the variance for the sample size. The more iterations are done per sample size, the more the mean will converge to the true grade of the image. The results of the plots for calculations of the homogeneity percentage and the graphs for the mean and standard deviations can be found in Appendix E. The results will be discussed in 6.4.

6.4 Summary

In the previous sections, for several cases the homogeneity percentage, their grade distribution and the chance of characterization of the true grade for a certain confidence interval. For all images, the standard deviations and mean are calculated for the increasing sample sizes. Their variance from the true grade is evaluated for relative percentages of 1%, 10% and 20%. This indicates that, for example, a true grade of 15% is estimated to be 15 ± 0.15%, 15 ± 1.5% or 15 ± 3%. As mentioned before the percentages are relative and do not display an absolute percentage. The results can be seen in Table 2, Table 3 and Table 4.

Relative percentages are used since absolute percentages can give a wrong impression. For example, comparing sample sizes for absolute 1% within the true grade, it differs if the true grade is 1% or 30%. For 1%, it lies between 0% and 2%, and for 30% it lies between 29% and 31%. For the last case, the relative difference is not significant, where the relative difference between 0% and 1% is enormous.

From these results, it is concluded that the homogeneity percentage does not correlate with the number of samples needed. If the %H increases, it does not indicate the number of samples needed to be within the confidence level will decrease. The number of samples is shown based upon the smallest grade (target grade) in the distribution since that one is hardest to estimate due to its low concentration. These grades are displayed in bold in the tables.

Table 2. Sample size within relative 1% of the true grade for confidence levels of 68%, 95% and 99%

Sample	%H	Grade distribution	Confidence level:		
			68% (1σ)	95% (2σ)	99% (3σ)
Case 1	100	40%, 30%, **30%**	90%	97%	99%
Case 2	98	70%, 15%, 10%, **5%**	99%	100%	100%
Case 3	97	97%, 2%, **1%**	100%	100%	100%
Nugget	0	99%, **1%**	100%	100%	100%
Vein	10	88%, **12%**	97%	99%	100%
Gneiss	29	47%, 27%, **26%**	92%	98%	99%
Chalk	55	80%, 17%, **3%**	99%	100%	100%
Granite	71	61%, 32%, **7%**	98%	100%	100%
Peridotite	85	66%, **34%**	88%	97%	99%

Table 3. Sample size within relative 10% of the true grade for confidence levels of 68%, 95% and 99%

Sample	%H	Grade distribution	Confidence level:		
			68% (1σ)	95% (2σ)	99% (3σ)
Case 1	100	40%, 30%, **30%**	8%	26%	43%
Case 2	98	70%, 15%, 10%, **5%**	42%	74%	86%
Case 3	97	97%, 2%, **1%**	78%	94%	97%
Nugget	0	99%, **1%**	79%	94%	97%
Vein	10	88%, **12%**	22%	53%	72%
Gneiss	29	47%, 27%, **26%**	10%	30%	49%
Chalk	55	80%, 17%, **3%**	55%	83%	92%
Granite	71	61%, 32%, **7%**	33%	67%	82%
Peridotite	85	66%, **34%**	7%	23%	40%

Table 4. Sample size within relative 20% of the true grade for confidence levels of 68%, 95% and 99%

Sample	%H	Grade distribution	Confidence level:		
			68% (1σ)	95% (2σ)	99% (3σ)
Case 1	100	40%, 30%, **30%**	2%	8%	17%
Case 2	98	70%, 15%, 10%, **5%**	15%	42%	61%
Case 3	97	97%, 2%, **1%**	48%	78%	89%
Nugget	0	99%, **1%**	49%	79%	89%
Vein	10	88%, **12%**	7%	22%	38%
Gneiss	29	47%, 27%, **26%**	3%	10%	19%
Chalk	55	80%, 17%, **3%**	24%	55%	74%
Granite	71	61%, 32%, **7%**	11%	33%	53%
Peridotite	85	66%, **34%**	2%	7%	14%

With relative margins, in Table 2 it is visible that being 1% within the true grade, for almost all the samples, the total sample size has a minimum close to the population size of 2500. This is reasonable since it would be hard to determine the exact grade. If the grade in the distribution is low, the number of samples needed for a 99% confidence level does not decrease fast. With a higher grade in the distribution, the number of samples decreases more rapidly, since that chance is higher to sample an element with an abundance of 30% than with 1%.

As mentioned before, no correlation is found between homogeneity percentages and the sample sizes. A reason for this is that in the used model, one sample is equal to one pixel. If the sample dimensions would be more significant, per sample could be calculated what %H is. Unfortunately, this cannot be done with the used model. Therefore, %H can only be used to determine the homogeneity of the total image. However, the tool is very useful for assessing the homogeneity within an image.

However, it can be seen that there is a trend between the grade distribution of the image and the sample size with its corresponding confidence level. For higher target grade, the sample size is lower than a low target grade. Table 5 gives an overview of the sample sizes focused on a target grade distribution from 1% to 99% and the sample sizes needed to be within relative 10% of that grade. It is calculated for confidence levels of 68%, 95% and 99%, which are equal to one, two and three standard deviations. All calculations assume a grid size of 50x50 pixel^2.

*Table 5. Grade distribution vs sample size (%) within relative 10% of **true grade (bold)** for multiple confidence levels.*

#	Grade distribution within image	Sample size (%)/confidence level:		
		68% (1σ)	95% (2σ)	99% (3σ)
1	99%, **1%**	78%	94%	97%
2	95%, **5%**	41%	74%	86%
3	90%, **10%**	25%	57%	76%
4	85%, **15%**	17%	46%	65%
5	80%, **20%**	13%	38%	57%
6	75%, **25%**	10%	31%	50%
7	70%, **30%**	8%	26%	44%
8	65%, **35%**	7%	22%	38%
9	60%, **40%**	5%	19%	35%
10	55%, **45%**	4%	15%	29%
11	50%, **50%**	4%	13%	25%
12	45%, **55%**	3%	11%	21%
13	40%, **60%**	3%	9%	19%
14	35%, **65%**	2%	8%	15%
15	30%, **70%**	2%	6%	13%
16	25%, **75%**	1%	5%	10%
17	20%, **80%**	1%	4%	8%
18	15%, **85%**	1%	3%	6%
19	10%, **90%**	< 1%	2%	4%
20	5%, **95%**	< 1%	1%	2%
21	1%, **99%**	< 1%	< 1%	< 1%

The sample size is displayed as a percentage of the total image (= 2500 pixels). The sample size for characterization of a 1% grade at a 99% confidence level needs to be 2429 (= 97%) to be within 10% of the true grade, which is between 0.9% and 1.1%. If the level of confidence decreases to 95%, the sample is equal to 2353 (= 94%), a decrease of only 3%. Of the confidence level decreases further to 68%, the required sample size is 1956 (= 78%). So, a difference of ±30% for the confidence level reduces the sample size with ±20% for a 50x50 pixel image. For a larger image, the sample size is expected to be even lower, but this will be evaluated in section 6.5.

The data from Table 5 is given as a graph in Figure 31. Here, it is visible that for a higher level of confidence (99%), the sample size is more extensive than with a lower confidence level (68%/95%). The function can be described as an exponential function which is steeper for a lower confidence level since it will need fewer samples with the same grade distribution. Therefore, it can be said that there is a correlation between the sample size and the grade distribution of the image. The more a target grade will decrease, the higher the sample size needs to be. For a target grade of 2% or lower, the sample size ratio needs to be at least 80%. For target grades above 90%, the required sample size ratio is lower than 5%.
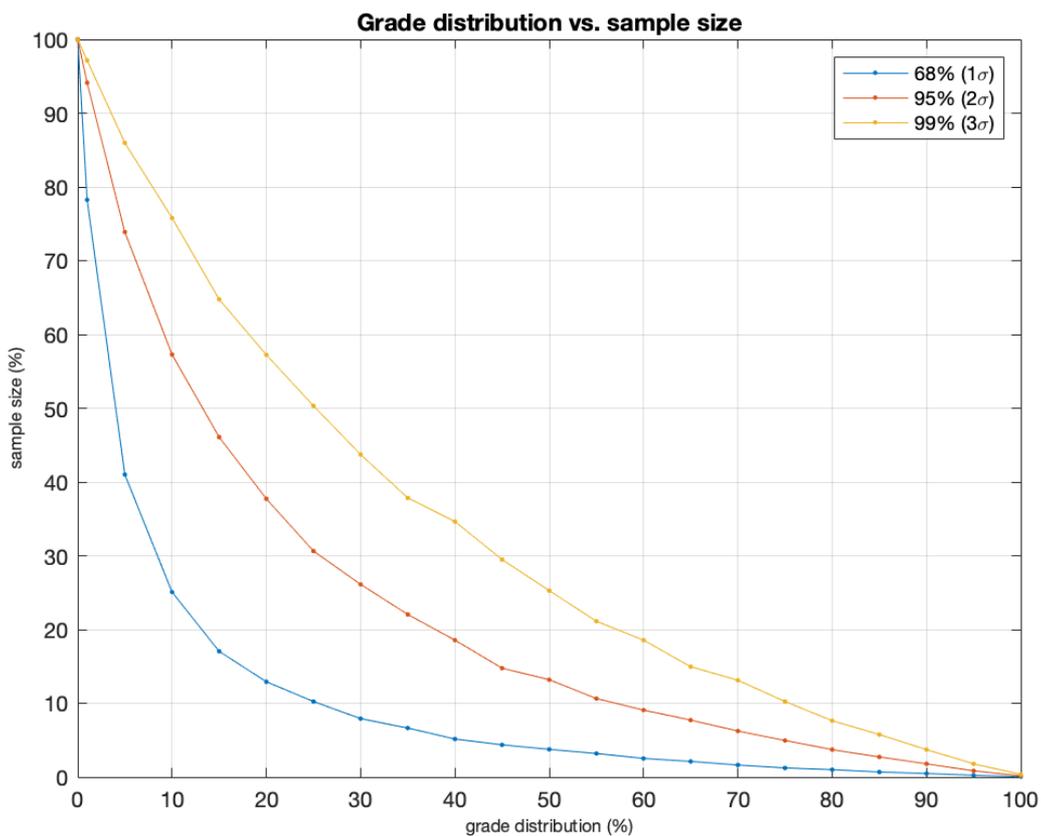
Figure 31. Graphical overview of grade distribution for a two-element material shown in Table 5.

6.5 Grid size versus sample size

The images and calculations done above are based upon a 50x50 pixel2 grid. Within this grid size, one can calculate the chance of determining the true elemental composition of the image. From the previous section, the lower the target grade, the higher the percental sample size. However, does this also relate to the grid size? If a sample size needs to be 80% of the total population, can it be said about all grid sizes or will the sample size ratio be lower with a larger grid size or vice versa?

To do so, the vein image of Figure 24 is evaluated. The grade distribution of the image is 88% and 12%. For a 50*50-pixel grid, this is equal to 2200 and 300 pixels. It is expected that with a lower grid size the relative sample size will increase. For example, 1% sample size of a 10*10-pixel grid indicates a sample size of 1 pixel. With only 1 pixel, no sufficient characterization can be done. A 1% sample size of a 50*50-pixel grid indicates a sample size of 25 pixels. With 25 samples, a basic characterization of the image can be done, based on the wanted level of confidence. So, with a sample size of 1%, the same accuracy cannot be achieved. It is expected that the higher the grid size, the lower the relative sample size ratio.

For different grid sizes, the vein structure is evaluated. For all grid sizes, a distribution of 88% and 12% is used which is evaluated for a 68%, 95% and 99% confidence level with relative margins of error of 1%, 10%, and 20%. The sample size is evaluated for the target grade of 12% since this is the lowest grade and therefore the hardest the characterize within the margins of error. Figure 32 gives a graphical overview of the grid sizes and the corresponding sample sizes. The used data can be found in Appendix D.
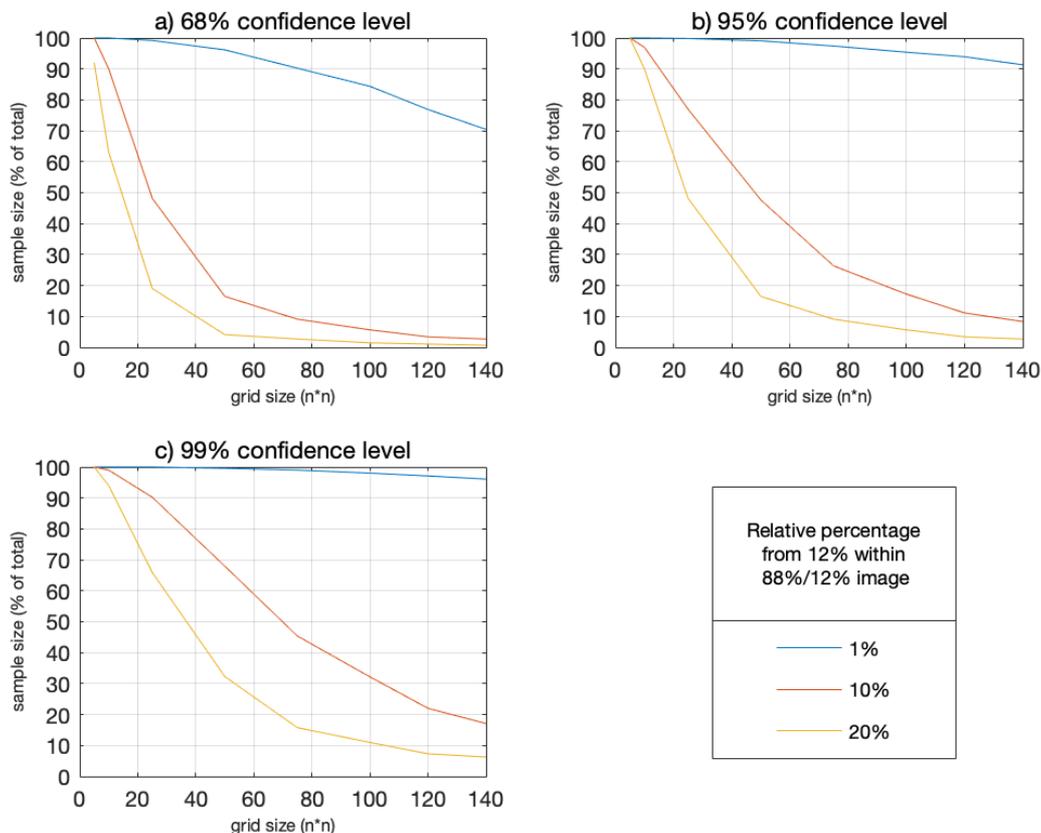
*Figure 32. Sample size percentage versus the grid size, evaluated for 5*5 grid up to a 140*140 pixels grid.*

For an increasing grid size, it is wise to know how much the relative sample size will decrease. To do so, an extrapolation can be made with the known data. This is shown in Figure 33, where the data with a 95% confidence level can be seen. Here, significant differences can be seen for the 1% and the 10%/20% margins of error. Where the margins of error of 10% and 20% are going downwards quickly to ±3%. For the 1% margin of error, the trend decreases slowly. At a grid size of 250*250, for a 10% and 20% margin of error, the sample size is circa 3% of the whole population. For a margin of error of 1%, this is much higher, circa 86%, which is a significant difference.

It can be said that the correlation between the sample and grid size is exponential, which is similar to sample size compared with the grade distribution in the previous section. For the 10% and 20% margin of error, after a grid size of 220*220, the relative sample size stays constant. It can be assumed that also the fitted line for 1% is exponential and will approach the same minimum. However, the grid size for this will be enormous, which can be clarified by the fact that a 1% margin of error is exact and therefore takes many measurements.

So, there is a correlation between the relative sample and grid size, which indicates relative fewer samples are needed when a more substantial surface or volume is characterized using LIBS. The results for Figure 33 are only for an 88% and 12% distribution of two components. For other grade distribution, the sample size will be higher or lower, depending on the number of elements with their distribution. With this case study, it is only proved that an increasing grid size will results in relatively lower sample size compared to the total population of the image.
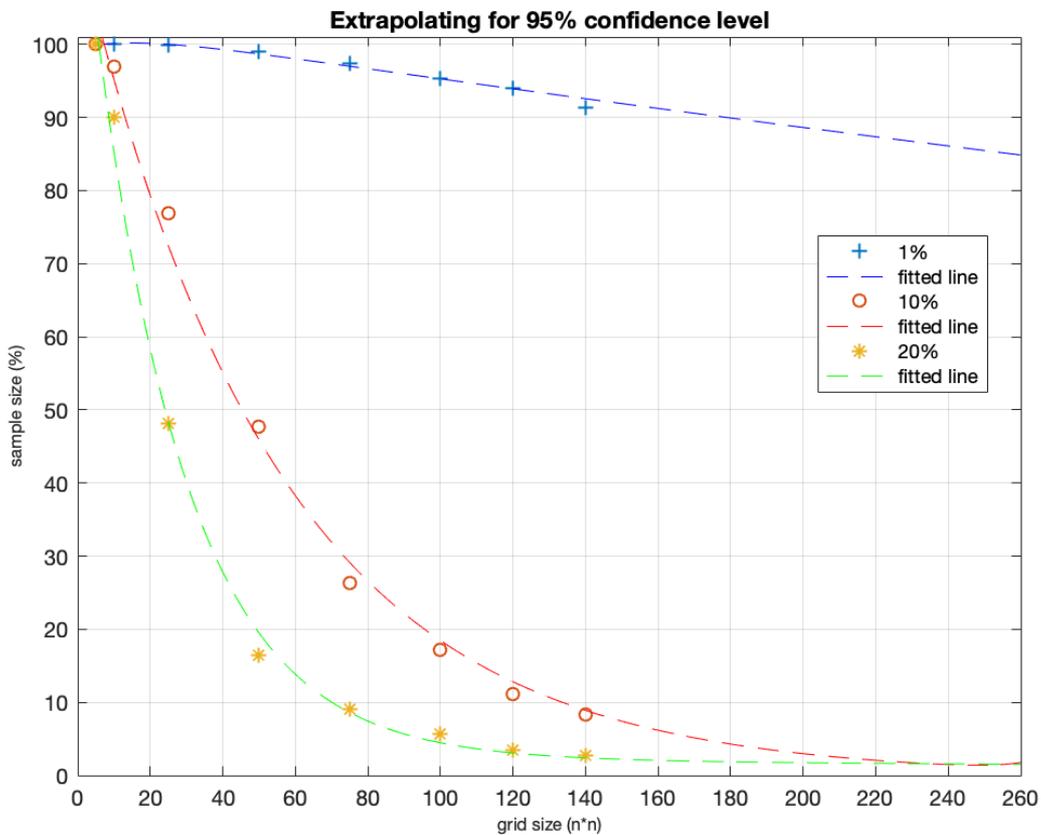
Figure 33. Extrapolation of the relative sample size compared with an increasing grid size.

6.6 Variogram and kriging

Kriging could be an option to evaluate the homogeneity of an image based on the samples taken, with the help of the range and the sill. To evaluate this, the samples from section 6.3 are evaluated using an (experimental) variogram which is used to recreate the image, and define the grade. For the four images, first, the sample percentage is determined using Table 5, which is evaluated for two elements, but will now also be used for three elements. A level of confidence of 95% is used. Table 6 gives an overview of the relative/absolute sample sizes.

Table 6. Overview of the required sample size based on the lowest target grade.

Image	Lowest target grade	Relative sample size	Absolute sample size
Gneiss	26% → 25%	31%	775
Chalk	3% → 5%	74%	1850
Granite	7% → 5%	74%	1850
Peridotite	34% → 35%	22%	550

For each image, a randomly selected number of the optimal absolute sample sizes is selected. From these selected values, a variogram is made which is defined as the variance of the difference between field values at two locations across realizations of the field [19]. These represent the spatial correlation between the sample points of the image. So, when the distance between a point increases, there will be a point where there is no spatial correlation, so no assumptions of the characterizations can be made.

Figure 34 shows an overview of the variograms for all images, where some differences can be distinguished at first sight. The variogram with the highest range is expected to be the most spatially correlated until that given lag distance. So, one can say that the smaller the range, the faster an image is spatially correlated over a given distance, so it should behave more homogeneous. If the range is broad, the correlation is higher, so the same elements are expected to be closer to each other.

For the evaluated cases, the variogram for gneiss has the highest range, but also the highest sill. This indicates the sample points are spatial correlated quite a lag distance. These values can be found in Table 7 below. Here, the partial sill is the sill value minus the nugget. The nugget is the value at which the variogram intercept the y-axis. A nugget effect indicates more homogeneity, since it indicates less spatial distribution between the samples.

Table 7. Overview of values of the range, sill and nugget.

Image	Range	(Partial) Sill	Nugget
Gneiss	19.3	0.55	-
Chalk	7.1	0.16	0.02
Granite	12.9	0.14	0.23
Peridotite	3.5	0.22	-
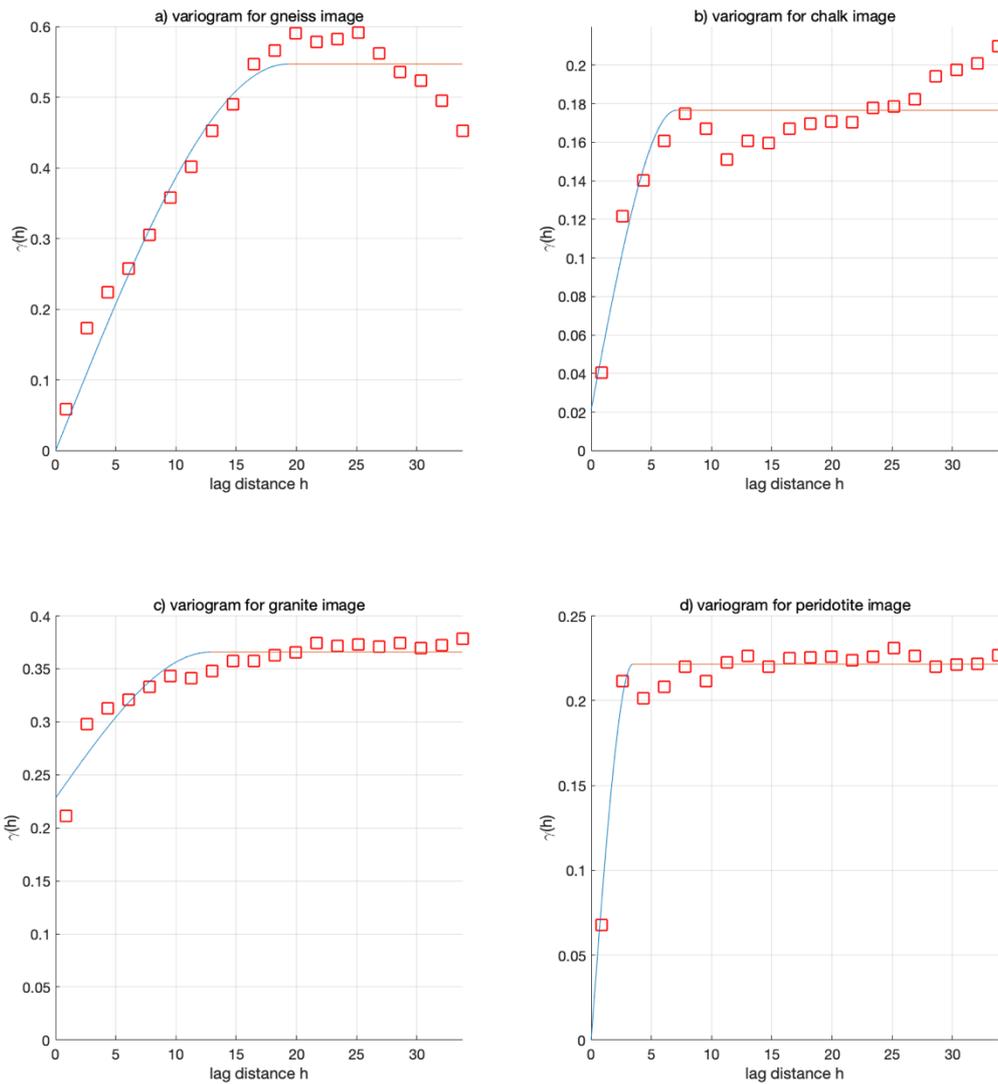
Figure 34. Fitted variograms for the a) gneiss, b) chalk, c) granite and d) peridotite images.

Lyman et al. (2011) state that the lower the sill and range are, the more homogeneous an image will be. Looking at Table 7 and Figure 34, this would indicate that the chalk and peridotite images will be more homogeneous than the gneiss and granite. Comparing this with the known homogeneity percentages, this is not valid. For the selected sample sizes of Table 6, the results of the kriging interpolation are shown in Figure 35. These images have been created using the `Kriging` function in MATLAB with input data from the variograms in Figure 34.

Comparing the kriging results with the original images, the interpolations are quite the same. The gneiss image shows the characteristic vein in the image, but can be a bit blurry looking at the other pixels. This also the case for all the other images, since it is interpolated and the images are more smoothened than the original ones, where more single pixels can be spotted.

Kriging can be used in order to generate an interpolation between sample points of an image. It could be used to get a first impression on the spatial distribution within certain sample spots with the help of the variogram. However, it can be concluded that it is not accurate since the kriging results are not similar to the results obtained with the image analysis tool [14].
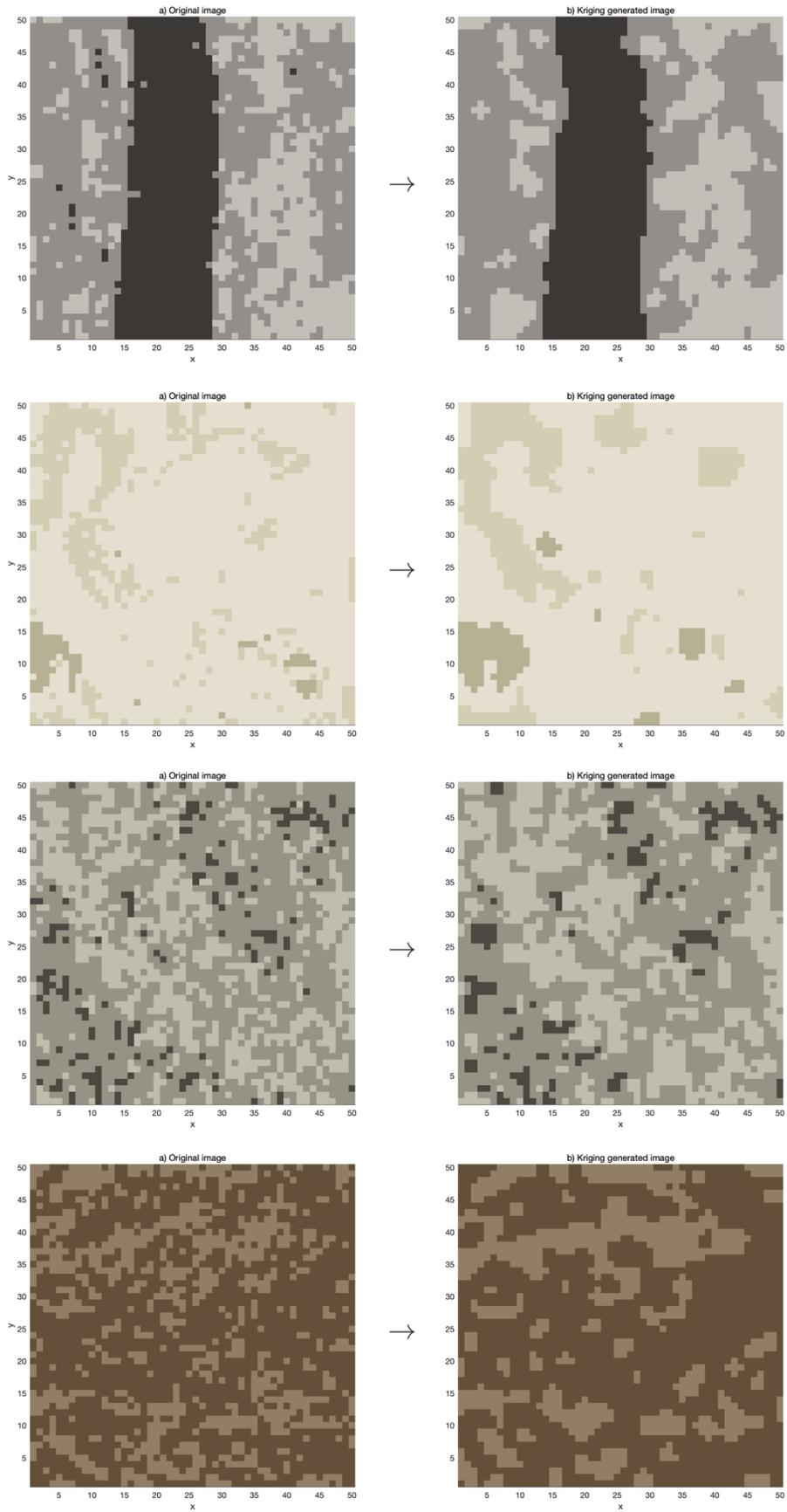
Figure 35. Kriging interpolation based upon samples from the original image. From top till bottom the gneiss, chalk, granite and peridotite image.

7. Discussion

The aim of this study was to investigate the relation between the homogeneity of a rock and the corresponding minimum sample size to reach a certain margin of error within a specified level of confidence. Different possibilities to encounter homo- and heterogeneity are discussed, for example, constitutional and distribution homogeneity. However, these options are not ideal for calculating and evaluating the percentage of homogeneity. The formulas need extra parameters, which include density and the grain size estimation of the throughput, which would difficult or not even possible within this context.

For different images, the homogeneity curves are calculated which are used to obtain a percentage of homogeneity. This is tested for several theoretical and real-life cases, where it proved to be a good manner to determine homogeneity within an n by n pixel grid. However, this cannot be used to determine a minimum sample size. Further, the standard deviation and mean is evaluated for increasing sample sizes compared with the total population. This resulted in graphs where the standard deviations are indeed decreasing if the sample size will be increased, but it is independent of homogeneity. This can then be used in order to determine margins of error compared to the target grade which needs to be characterized within the entire grid.

Further, the correlation between the grade distribution and sample size is shown. For smaller target grades, more samples are needed in order to reach the same margin of error. For a more substantial target grade the required sample size will decrease. However, this is evaluated for two elements were the results of an increasing number of elements are expected to be different. If the grid size (n by n) will be increased, a relatively smaller proportion of the samples is needed to get the same margins of error within the same levels of confidence. Kriging could be used to evaluate the spatial correlation of the distribution when sample points are known. Within a grid environment, this can be useful, but sample coordinates are required in order to create a variogram.

Overall, for specific cases, the minimum sample size can be calculated. However, in a real-life mining environment, the subsurface is not known, as is the distribution or composition of that material. Therefore, it is unlikely that a standard formula can be determined to assess the sample size based on specific parameters as the rate of homogeneity since this is already hard to determine at itself. The results of this study are valid for their specific case studies, which is a 50 x 50 pixel2 grid with a maximum of four elements. Within a rock, much more particles and elements are available, making it difficult to use the results from this study in real cases.

This is also the hardest part of this study. No natural material or rock has the same composition. For LIBS measurements, only the surface is characterized. What is in the subsurface can only be guessed since there is no correlation between the surface and the volume for the majority of the rocks. Sampling within the mining industry is always tricky and incorporates risk since it is hard to give a minimum sample size. The total composition is not known, which makes it is almost impossible to assume the minimum sample size.

In a future study, it is recommended to use more elemental compositions and different grid sizes. Also, no correlation between the percentage of homogeneity and the grade distribution was found, which can be valuable for determining the minimum sample size. If the rate of homo- or heterogeneity can be determined for more complex structures, calculating a minimum sample size can be a step closer. This study had limited time to incorporate this, but it could be done in the future.

8. Conclusion

For a long time, the theory of sampling has been studied in order to assess the problem of determining the required sample size for an image or material. This study has resulted in the findings that the spatial distribution of elements in a sample can increase or decrease the relative sample size of an image. It has been shown that more homogeneous images require fewer samples than, for example, a vein structure. Within different levels of confidence and margins of errors, the sample sizes of the images vary, where the lower the margin of error and the higher the level of confidence, the more samples one need to take. This is shown with the help of modelling several case studies in MATLAB. Also, the homogeneity percentage is calculated with the help of an image analysis tool.

Interpreting these results, it is possible to determine the required sample size for an image, if the right assumption will be made. These include a known fixed grid size and a predefined grade distribution. With these assumptions, the minimum sample sizes can be calculated within the levels of confidence and margins of error. In real-life these situations this is not realistic.

The grid size, surface area or volume in real life situation is hard to determine since the boundary conditions are not constant. Also, the grade distribution is not known, and these are likely to be much more complicated than the case studies within the work. However, within a LIBS grid, similar to Figure 17, the percentage of homogeneity can be assessed, and the grade distribution could be used, and such a sample could be used to assess the overall composition, but this is not recommended since the surface area is minimal and not continuous through the whole image.

No correlation has been found between the percentage of homogeneity, calculated with the image analysis tool [14], and the minimum sample size. This indicates that the distribution is not needed for determining the sample size. However, this is only valid for the used image analysis tool, fixed boundary conditions, a known grid size and grade distribution. In real life, these parameters are mostly hard to known.

For the grade distribution and sample size, a correlation was found. This has also been done for comparing an increasing grid size and the relative sample size between a certain margin of error and level of confidence. These correlations are exponential, which means for doubling the grid size or grade distribution, the sample size will decrease. This can be valuable and needs further research for more complex grade distributions with more than two elements and grid sizes exceeding 1000 x 1000 pixels.

It was known that answering the question on a minimum sample size based upon a specific rate of homo- or heterogeneity would be hard to answer. Evaluating the homogeneity of a surface itself is already very difficult, and many studies have been carried out trying to answer the question. Some good work has been done, but the mining industry will always be different, and one research cannot be used for a wide variety of other cases. Therefore, this study can be useful with simple and basic images, but for more complex structures more research is needed to answer what the minimum sample size will be.

LIBS can be used very good for detection of minerals, but it will hard to know the minimum sample size for these measurements. In the future, it would be perfect to have a tool that evaluates the rate of homogeneity and the grade distribution real-time so the sample size can be adjusted automatically by the system. Therefore, an automated system to detect the elemental composition is needed, and extensive research needs to carried out.

9. Acknowledgements

Bibliography

[1] J. J. Kiptarus, A. M. Muumbo, A. B. Makokha and S. K. Kimutai, "Characterization of Selected Mineral Ores in the Eastern Zone of Kenya: Case Study of Mwingi North Constituency in Kitui County," *International Journal of Mining Engineering and Mineral Processing,* vol. 4, no. 1, pp. 8-17, 2015.

[2] N. Khajehzadeh and T. K. Kauppinen, "Fast mineral identification using elemental LIBS technique," *IFAC-PapersOnLine,* vol. 48, no. 17, pp. 119-124, 2015.

[3] Real Time Mining, "Real-Time Optimization of the Extraction and the Logistics Process in Highly Complex Geological and Selective Mining Settings," 2017. [Online]. Available: https://www.realtime-mining.eu/. [Accessed 3 October 2018].

[4] N. Khajehzadeh, O. Haavisto and L. Koresaar, "On-stream and quantitative mineral identification of tailing slurries using LIBS technique," *Minerals Engineering,* vol. 98, no. 1, pp. 101-109, 2016.

[5] D. A. Cremers, F.-Y. Yueh, J. P. Singh and H. Zhang, "Laser-Induced Breakdown Spectroscopy, Elemental Analysis," in *Encyclopedia of Analytical Chemistry: Applications, Theory and Instrumentation*, John Wiley & Sons, Ltd., 2000, pp. 50-62.

[6] M. Dalm and M. Buxton, "Characterizing the economic value of an epithermal Au-Ag ore with Laser Induced Breakdown Spectroscopy (LIBS): Possibilities and Limitations," Delft University of Technology, Faculty of Civil Engineering and Geosciences, Resource Engineering section., Delft, 2015.

[7] M. Gaft, I. Sapir-Sofer, H. Modiano and R. Stana, "Laser induced breakdown spectroscopy for bulk minerals online analyses," *Spectrochimica Acta Part B: Atomic Spectroscopy,* vol. 62, no. 12, pp. 1496-1503, 2007.

[8] M. Abzalov, "Introduction to the Theory of Sampling," in *Applied Mining Geology*, Mount Claremont, WA, Australia, Springer, 2016, pp. 119-134.

[9] J. E. Bartlett, J. W. Kotrlik and C. C. Higgins, "Organizational Research: Determining Appropriate Sample Size in Survey Research," *Information Technology, Learning, and Performance Journal,* vol. 1, no. 19, pp. 43-50, 2001.

[10] S. Seiler, "Surface XRF Mapping for Intraparticle Heterogeneity Assessment and Particle Grade Estimation," Universidad de la República; The University of British Columbia, Vancouver, 2015.

[11] P. J. Fitch, M. A. Lovell, S. J. Davies, T. Pritchard and P. K. Harvey, "An integrated and quantitative approach to petrophysical heterogeneity," *Marine and Petroleum Geology,* vol. 63, pp. 82-96, 2015.

[12] K. H. Esbensen, "Materials Properties: Heterogeneity and Appropriate Sampling Modes," *Journal of AOAC International,* vol. 98, no. 2, pp. 269-274, 2015.

[13] P. Gy, in *Sampling for Analytical Purposes*, Chichester, John Wiley & Sons, Ltd., 1998, pp. 63-68.

[14] G. J. Lyman, "In situ and particulate material heterogeneity," Materials Sampling & Consulting, Australia, Santiago, 2011.

[15] A. Journel and C. Huijbreghts, in *Mining Geostatistics*, Academic Press, 1978.

[16] G. Matheron, "Principles of geostatistics," *Economic Geology,* vol. 58, no. 8, pp. 1246-1266, 1962.

[17] Khan Academy, "Population and sample standard deviation review," 12 May 2016. [Online]. Available: https://www.khanacademy.org/math/statistics-probability/summarizing-quantitative-data/variance-standard-deviation-sample/a/population-and-sample-standard-deviation-review. [Accessed 2018 November 7].

[18] D. T. Kaplan, "Resampling Stats in MATLAB," Macalestor College; Department of Mathematics and Computer Science; St. Paul, Minesota, USA, 29 April 1996. [Online]. Available: https://www.macalester.edu/~kaplan/Resampling. [Accessed 24 October 2018].

[19] N. Cressie, "Statistics for spatial data," *Wiley Interscience,* 1993.

[20] D. Cremers and L. J. Radziemski, in *Handbook of Laser-Induced Breakdown Spectroscopy*, Chichester, Wiley & Sons Ltd., 2013, p. 432.

[21] P. Minkkinen, "Theory of Sampling: General principles for sampling heterogeneous materials," *Reliable Data for Waste Management,* pp. 25-26, 2008.

[22] Pacific Northwest; National Laboratory, "Kriging Variogram Model," U.S. Department of Energy, 27 10 2017. [Online]. Available: https://vsp.pnnl.gov/help/vsample/Kriging_Variogram_Model.htm. [Accessed 15 10 2018].

[23] L. de Moura França, J. M. Amigo, C. Cairós, M. Bautista and M. F. Pimentel, "Evaluation and assessment of homogeneity in images. Part 1: Unique homogeneity percentage for binary images," *Chemometrics and Intelligent Laboratory Systems,* vol. 171, pp. 26-39, 2017.

[24] N. Cavalcante da Silva, L. de Moura França, J. M. Amigo, M. Bautista and M. F. Pimentel, " Evaluation and assessment of homogeneity in images. Part 2: Homogeneity assessment on single channel non-binary images. Blending end-point detection as example," *Chemometrics and Intelligent Laboratory Systems,* vol. 180, pp. 15-25, 2018.

[25] Wikipedia.org, "68–95–99.7 rule," 18 October 2018. [Online]. Available: https://en.wikipedia.org/wiki/68%E2%80%9395%E2%80%9399.7_rule. [Accessed 23 October 2018].

[26] Encyclopædia Britannica, Inc., in *Encyclopædia Britannica*, London, 2011.

[27] IHC Merwede, "Concept of implementation LIBS in the mining industry," IHC Merwede, Kinderdijk, 2018.

[28] M. Sandtke, "Drill Core Element Mapping," Spectral Industries, 10 April 2018. [Online]. Available: https://www.spectralindustries.com/drill-core-element-mapping/. [Accessed 24 October 2018].

Appendices

A. Theory of constitutional and distribution heterogeneity

The contribution made to the heterogeneity of lot L by some unknown unit Um:

Lot L, the subject of the study, can be regarded in general terms as a population of unspecified units Um that can be defined alter as the case requires. A sit he 'critical component' or analyte, the component of interest. References to the grade or concentration of component A are to its actual but unknown grade, not to some estimate of it. The following definitions are made:

N_U number of units U_m in lot L

M_m mass of the unit U_m

M_L mass of lot L. It is the sum of the masses M_m of the N_U units of U_m

M_{m*} mass of the mean unit U_{m*} of lot L, defined as the mean of the masses M_m

a_m the grade of the analyte A in unit U_m (i.e. the proportion by mass of A in U_m)

a_L the grade if analyte A in lot L (i.e. the proportion by mass of A in L)

h_m the contribution of the heterogeneity of lot L made by U_m, defined as follows:

$$h_i = \frac{(a_i - a_L)}{a_L} * \frac{M_i}{M_{i*}} \; with \; a_L = \frac{\sum_m a_m M_m}{\sum_m M_m} \; and \; M_{m*} = \frac{M_L}{N_U}$$

The constitutional Heterogeneity CH_L of Lot L: $U_m = F_i$:

Initially, the scale of observation will be such that unit U_m is a fragment, a molecule or an ion F_i. The following are thus defined:

h_i the contribution of the fragment F_i to the heterogeneity if L

$$h_i = \frac{(a_i - a_L)}{a_L} * \frac{M_i}{M_{i*}} \; with \; i = 1,2, \dots, N_F \; and \; M_{i*} = \frac{M_L}{N_F}$$

CH_L the constitutional heterogeneity of lot L defined as the variance of h_i:
$CH_L = s^2(h_i)$, nothing that $m(h_i) = 0$

As long as the fragments, molecules, ions F_i remain unaltered the constitutional heterogeneity CH_L is an intrinsic property of L.

Distributional heterogeneity DH_L of lot L: $U_m = I_n$:

The scale of observation is now that at which the unit U_m is a group I_n of neighboring fragments, molecules or ions. The following can be defined:

h_n the contribution of the group I_n to the heterogeneity if L, defined as:

$$h_n = \frac{(a_n - a_L)}{a_L} * \frac{M_n}{M_{n*}} \; with \; n = 1,2, \dots, N_I \; and \; M_{n*} = \frac{M_L}{N_I}$$

DH_L the distributional heterogeneity of fragments F_i within L, defined as:
$DH_L = s^2(h_n)$, nothing that $m(h_n) = 0$.

Unlike the fragments F_i, the groups I_n of fragments can alter. Any mixing, homogenizing or segregation alters the distribution of the fragments between the groups and thus the value DH_L. Mixing and homogenizing reduce DH_L; segregation increases it.

From: Sampling for Analytical Purposes, Pierre Gy (1998)

B. Mineralogical assays of the tailing samples using LIBS

Mineral	Sample (%)													
	T1	T2	T3	T4	T5	T6	T7	T8	T9	T10	T11	T12	T13	T14
Quartz	34.8	40	30.4	45.1	60.8	52	44.8	37.1	48.2	59.3	61.5	54.4	38	46.6
K-feldspar	2.2	3.5	3.1	2.4	2.1	2.3	2.4	2.2	1.5	2.6	2.4	2.8	2.4	1.8
Aegirine-augite	3	2.7	4.3	2.9	1.5	2.1	1.9	3.2	2.1	1.4	1.4	1.5	2.5	1.1
Biotite	1.9	1.9	2.1	4	4.2	3.5	3.5	2.9	2	1.9	1.7	1.7	1.6	1.3
Galuconite	0.1	0.2	1.1	1.8	2.5	1.3	1.3	0.6	0.1	0.2	0.2	0.4	0.3	0.5
Stilpnomelane	4.3	4.2	3.8	4	2.1	2.8	2.6	3.7	5.3	3	1.8	1.9	3.2	3.6
Actinolite	0.1	0.2	0	0	0	0.1	0.1	0.1	0.1	0.2	0.2	0.3	0.5	0.3
Ferrorichterite	8.6	8.1	2.5	3.7	1.9	3.4	3.5	7.7	9.1	3.2	2.1	2.3	3.6	1.9
Magnetite	42	37.1	47.2	31.1	17.6	26	32.3	39.1	29.1	19.6	21	27	39	35.6
Hematite	1.7	1	4.3	3.8	5.8	5	6.2	2.4	1.3	7	6.6	6.3	7	5
Unknown	0.9	0.9	0.9	0.8	1.2	1	1	0.8	0.8	1.3	1	1.3	1.1	1.9

C. Formula for calculating the smallest sample size

Sample statistic	Population size	Sample size formula
Mean	Known	$n = \dfrac{z^2\sigma(\frac{N}{N-1})}{e^2 + \frac{z^2\sigma^2}{(N-1)}}, \quad \sigma^2 \to pop^n\ var.$
Mean	Unknown	$n = \dfrac{z^2\sigma^2}{e^2}$
Proportion	Known	$n = \dfrac{z^2pq + e^2}{\frac{z^2\ pq}{N} + e^2}$
Proportion	Unknown	$n = \dfrac{z^2\ pq + e^2}{e^2}$

D. Data sample size/grid size versus a constant grade

Table 8. Overview of increasing grid sizes with corresponding sample size for different levels of confidence and margins of error. Results are displayed in both absolute value and the percentage to the whole population.

Grid size	Level of confidence	Margin of error (relative to 12%)					
		1%		*10%*		*20%*	
5*5	*68%*	25	100%	25	100%	23	92%
	95%	25	100%	25	100%	25	100%
	99%	25	100%	25	100%	25	100%
10*10	*68%*	100	100%	90	90%	63	63%
	95%	100	100%	97	97%	90	90%
	99%	100	100%	99	99%	94	94%
25*25	*68%*	620	99%	301	48%	119	19%
	95%	624	100%	481	77%	301	48%
	99%	625	100%	564	90%	412	66%
50*50	*68%*	2404	96%	412	16%	103	4%
	95%	2477	99%	1191	48%	412	16%
	99%	2490	100%	1699	68%	807	32%
75*75	*68%*	5076	90%	513	9%	152	3%
	95%	5479	97%	1482	26%	513	9%
	99%	5570	99%	2553	45%	887	16%
100*100	*68%*	8437	84%	567	6%	147	1%
	95%	9539	95%	1722	17%	567	6%
	99%	9805	98%	3219	32%	1099	11%
120*120	*68%*	11071	77%	490	3%	155	1%
	95%	13528	94%	1605	11%	490	3%
	99%	13985	97%	3171	22%	1054	7%
140*140	*68%*	13810	70%	529	3%	135	1%
	95%	17901	91%	1638	8%	529	3%
	99%	18835	96%	3354	17%	1229	6%

E. Plots
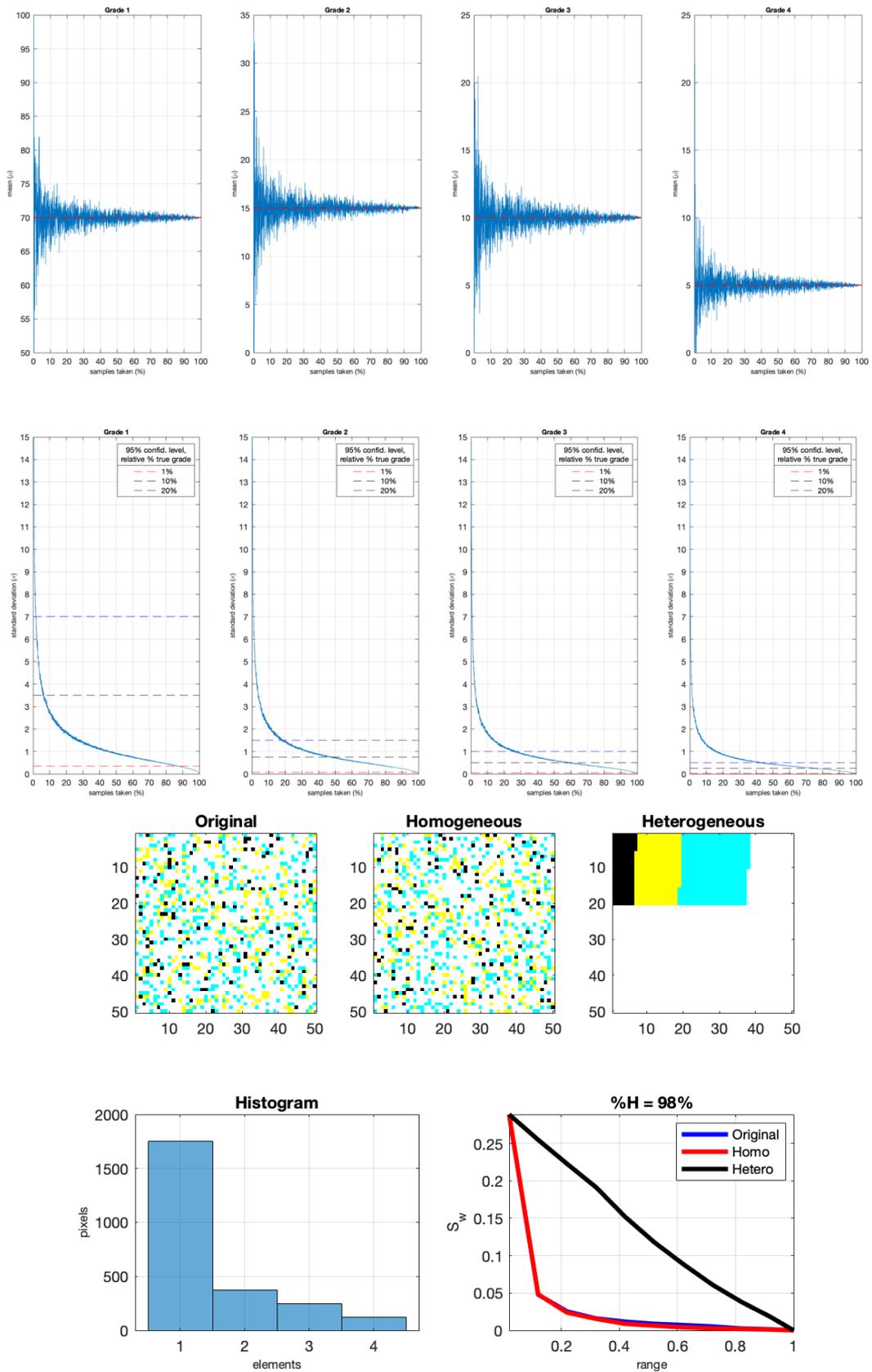
Figure 36. Mean, standard deviation and homogeneity curve of Case 2 (70%, 15%, 10%, 5%) in section 6.2.
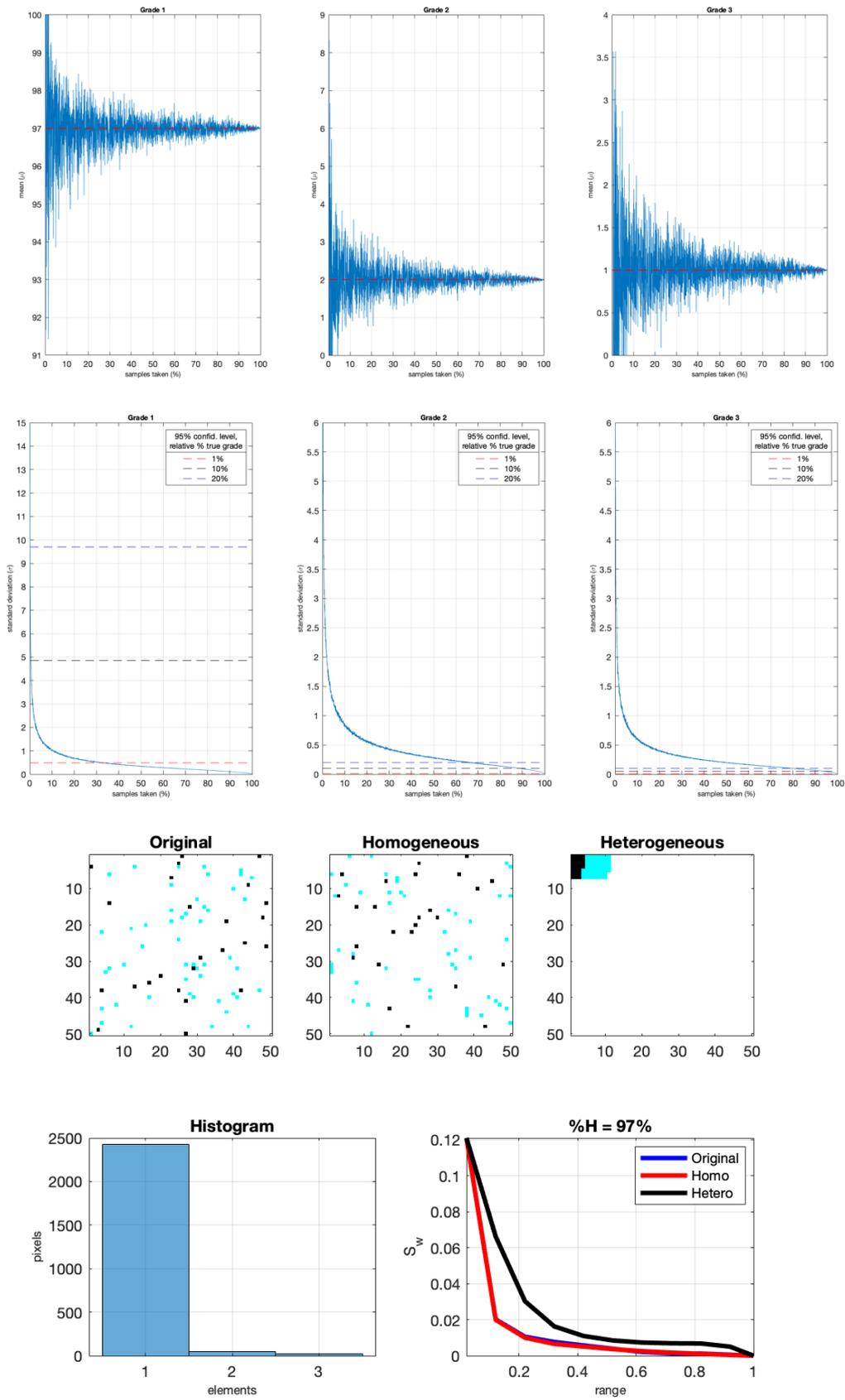
Figure 37. Mean, standard deviation and homogeneity curve of Case 3 (97%, 2%, 1%) in section 6.2.
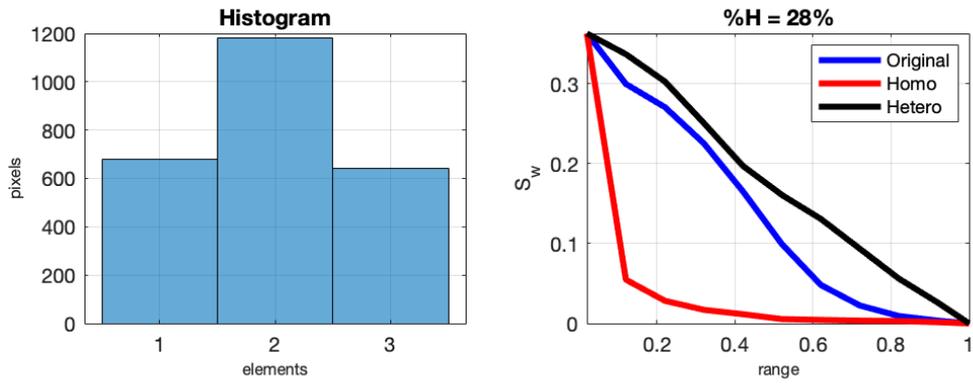
Figure 41. Histogram for distribution and homogeneity curve for the gneiss rock sample.
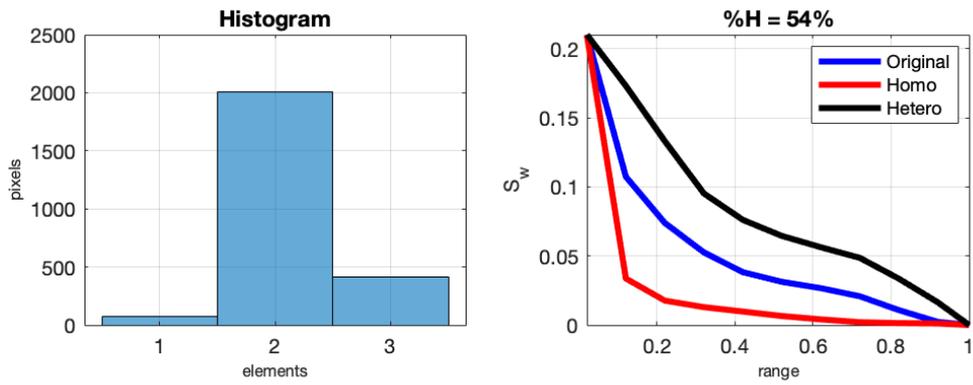
Figure 41. Histogram for distribution and homogeneity curve for the chalk rock sample.
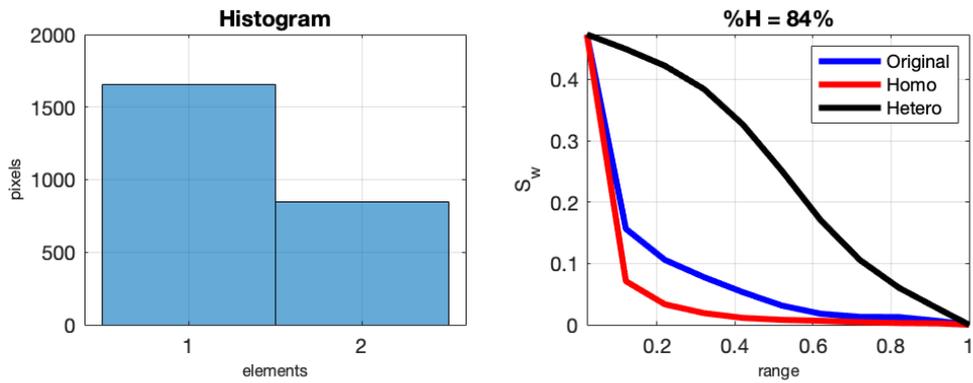
Figure 41. Histogram for distribution and homogeneity curve for the peridotite rock sample.
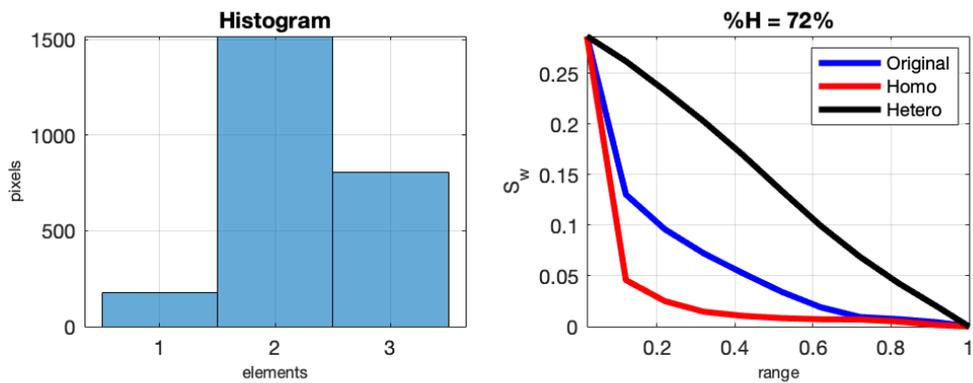
Figure 41. Histogram for distribution and homogeneity curve for the granite rock sample.
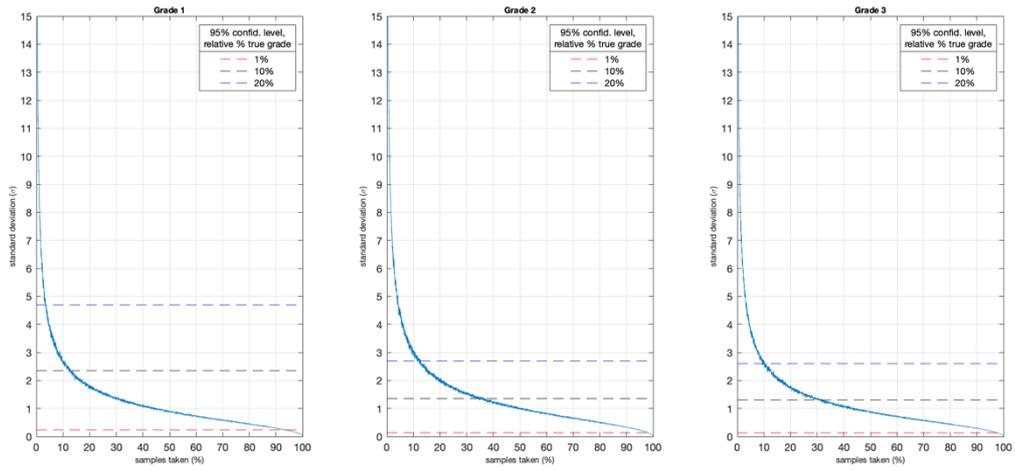
Figure 42. Standard deviations for Gneiss image, with grade distribution 47%, 27%, 26%.
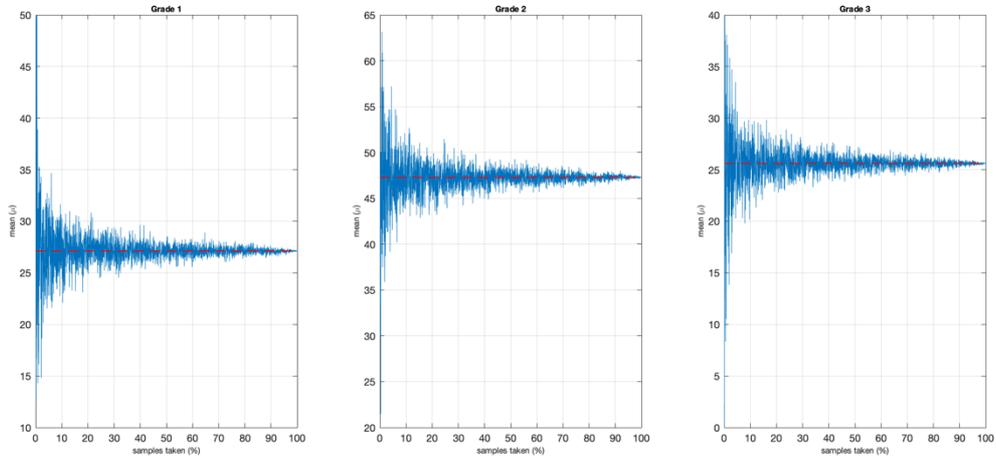
Figure 43. Variations of the mean for Gneiss image, with grade distribution 47%, 27%, 26%.
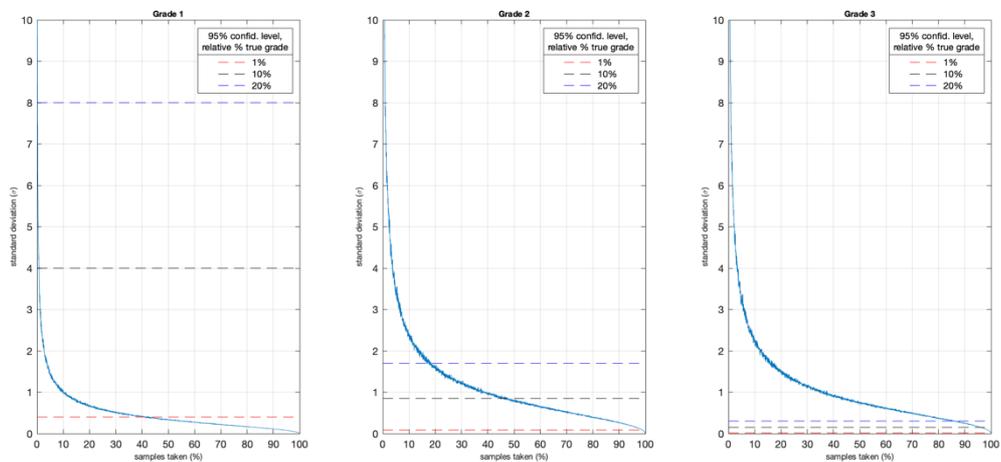
Figure 44. Standard deviations for Chalk image, with grade distribution 80%, 17%, 3%.

45
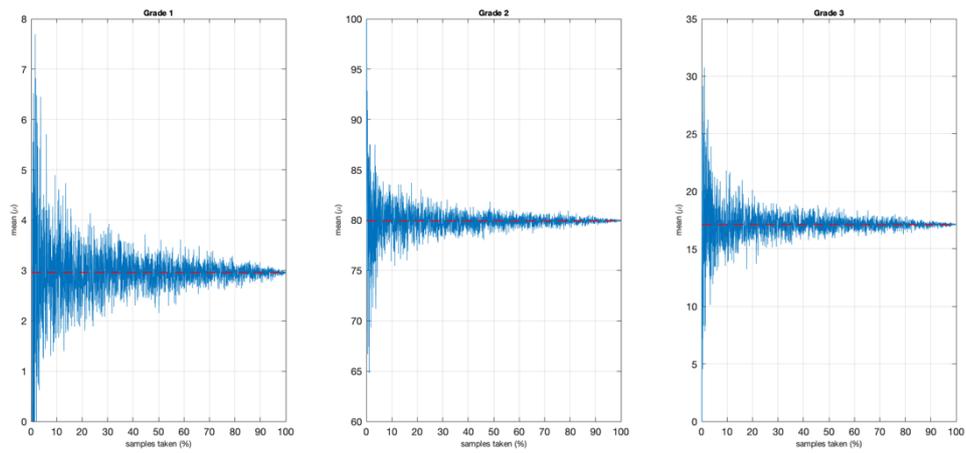
Figure 45. Variations of the mean for Chalk image, with grade distribution 80%, 17%, 3%.
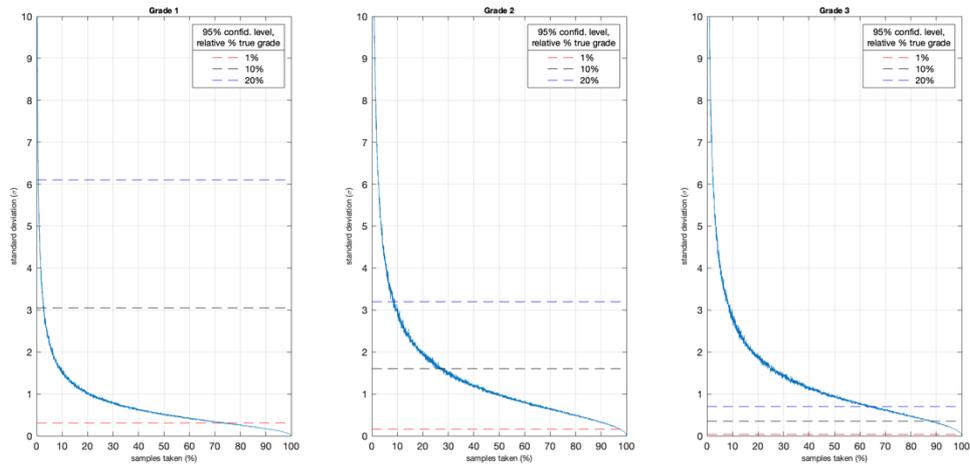
Figure 46. Standard deviations for Granite image, with grade distribution 61%, 32%, 7%.
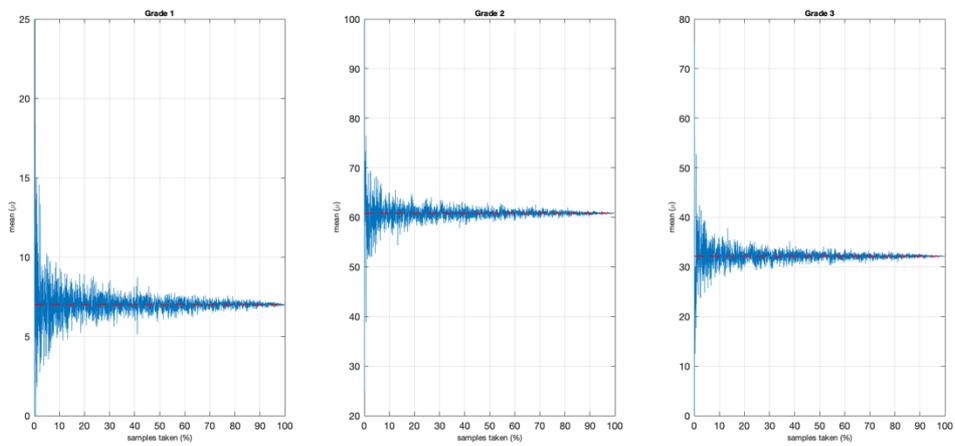
Figure 47Variations of the mean for Granite image, with grade distribution 61%, 32%, 7%.
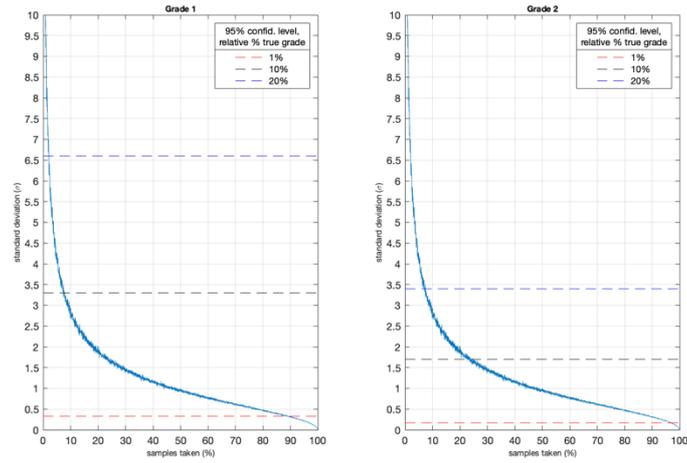
Figure 48. Standard deviations for Peridotite image, with grade distribution 66%, 34%.
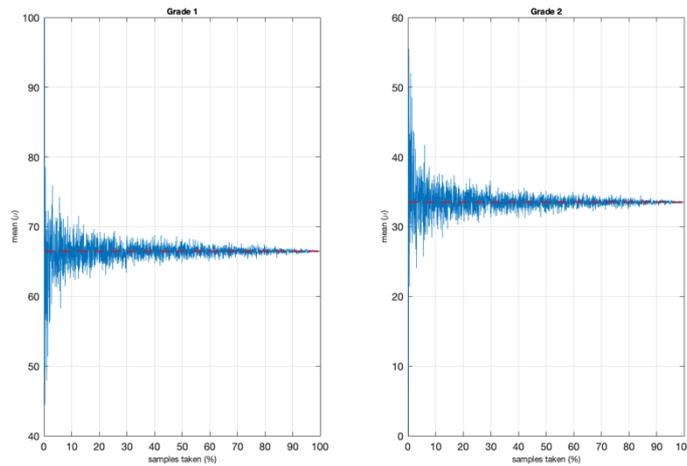
Figure 49. Variations of the mean for Peridotite image, with grade distribution 66%, 34%.

F. MATLAB script manual

Generating the figures in this study, several MATLAB scripts are used. This section explains how these scripts can be used to obtain the same results. The scripts are provided with this study as zip file and can be requested by the author. Within the scripts, a description can be found including which inputs and output it generates.

Most of the times, the input image needs to be a mono-channel matrix. This indicates an n by m matrix with positive integer values, like 1, 2, 3, 23, etc.

Generate an image:
`Fig2pix.m` and `griddistribution.m` can be used to generate an image from a theoretical and real-life source.

Standard deviation and mean:
`Samplesd.m` and `samplemean.m` can be used to calculate the standard deviation and/or mean from a matrix input; for example, generated with `fig2pix.m` or `griddistribution.m`

Homogeneity percentage:
`Homogeneitycurve.m` can be used to gather three images of the original and generated homo- and heterogeneous images to create homogeneity curves and determine the percentage.
Grade calculation:
To calculate the grade of a matrix input, `gradecalc.m` can be used. All matrix sizes and composition can be inserted. The script returns the grade distribution in percentages per element.

Sample size:
The required sample size is based on the standard deviation from an inserted grade. The lower the desired margin of error, the lower standard deviation is required. `Samplesize.m` can be used to determine the minimum sample size using the standard deviations generated with `samplesd.m`.

All in calculation:
`Samplesize2.m` can be used to generate a minimum sample size with a mono-channel matrix input and a relative margin of error from the target grade.

Variogram and kriging:
For calculating the variogram and kriging output, `kriging_sample.m` is used. This is not in a function as the scripts above. It is divided in three sections, which have to executed chronologically. A mono-channel matrix needs to be inserted and the number of samples. In the second part, the initial sill, range and nugget can be inserted to generate and modify the variogram. If the variogram is fitted, the kriging result can be obtained by running the third section of the script.

Random points with coordinates:
For kriging random points need to be generated with the corresponding x and y coordinate. Samplegrid.m generated a n number of samples with its corresponding coordinates. This is used within `kriging_sample.m`.